Published for SISSA by Springer

Received: *September 11, 2015*
Accepted: *October 20, 2015*
Published: *November 11, 2015*

XCone: N-jettiness as an exclusive cone jet algorithm

Iain W. Stewart,[a] **Frank J. Tackmann,**[b] **Jesse Thaler,**[a] **Christopher K. Vermilion**[c] **and Thomas F. Wilkason**[a]

[a] *Center for Theoretical Physics, Massachusetts Institute of Technology, Cambridge, MA 02139, U.S.A.*

[b] *Theory Group, Deutsches Elektronen-Synchrotron (DESY), D-22607 Hamburg, Germany*

[c] *Ernest Orlando Lawrence Berkeley National Laboratory, University of California, Berkeley, CA 94720, U.S.A.*

E-mail: iains@mit.edu, frank.tackmann@desy.de, jthaler@mit.edu, christopher.vermilion@gmail.com, tjwilk@mit.edu

Abstract: We introduce a new jet algorithm called XCone, for eXclusive Cone, which is based on minimizing the event shape N-jettiness. Because N-jettiness partitions every event into N jet regions and a beam region, XCone is an exclusive jet algorithm that always returns a fixed number of jets. We use a new "conical geometric" measure for which well-separated jets are bounded by circles of radius R in the rapidity-azimuth plane, while overlapping jet regions automatically form nearest-neighbor "clover jets". This avoids the split/merge criteria needed in inclusive cone algorithms. A key feature of XCone is that it smoothly transitions between the resolved regime where the N signal jets of interest are well separated and the boosted regime where they overlap. The returned value of N-jettiness also provides a quality criterion of how N-jet-like the event looks. We also discuss the N-jettiness factorization theorems that occur for various jet measures, which can be used to compute the associated exclusive N-jet cross sections. In a companion paper [1], the physics potential of XCone is demonstrated using the examples of dijet resonances, Higgs decays to bottom quarks, and all-hadronic top pairs.

Keywords: Jets, QCD Phenomenology

ArXiv ePrint: 1508.01516

doi:10.1007/JHEP11(2015)072

JHEP11(2015)072

Contents

1 Introduction **1**

2 *N*-jettiness as a jet algorithm **4**

3 Choice of measure **6**
- 3.1 The conical measure 7
- 3.2 The geometric measure 10
- 3.3 The conical geometric measure 12
- 3.4 The XCone default measure 13

4 Details of the XCone algorithm **14**
- 4.1 One-pass minimization 14
- 4.2 Update step for general measures 16
- 4.3 Seed axes for one-pass minimization 17

5 *N*-jettiness factorization with various measures **20**
- 5.1 Separating into jet and beam regions 20
- 5.2 Categorizing measures by power counting 22
- 5.3 Impact of axes minimization 23
- 5.4 Hadronic and partonic momentum conservation 24
- 5.5 Convolutions from transverse momentum recoil 26
- 5.6 Factorization theorems for N-jettiness 28

6 Conclusions **31**

JHEP11(2015)072

1 Introduction

Collisions at the Large Hadron Collider (LHC) are dominated by jets, collimated sprays of hadrons arising from the fragmentation of energetic quarks and gluons. Jets are crucial to connect the observed hadronic final state to the short-distance hard interaction. Fundamentally, the definition of a hadronic jet is ambiguous, since there is no unique way to map color-singlet hadrons to color-carrying partons. Moreover, different physics applications can benefit from different jet definitions. For these reasons, a wide variety of jet algorithms have been proposed to identify and study jets [2, 3], though currently, most LHC measurements involve jets clustered with the anti-k_T algorithm [4].

In this paper, we present a new jet algorithm that we call "XCone". It is based on minimizing the event shape N-jettiness [5] and uses developments from the jet shape N-subjettiness [6, 7]. The key feature is that N-jettiness defines an *exclusive cone* jet algorithm. Like the exclusive k_T algorithm [8], our XCone algorithm returns a fixed number of jets, relevant for physics applications where the number of jets is known in advance. Like

anti-k_T jets [4], XCone jets are nearly conical for well-separated jets, such that they have fixed active jet areas [9, 10]. Typically, when using other jet algorithms, the boosted regime of overlapping jets requires separate analysis strategies using fat jets with substructure [11–14]. In contrast, with XCone the jets remain resolved even when jets are overlapping in the boosted regime. In this way, XCone smoothly interpolates between the resolved regime of widely-separated jets and the boosted regime of collimated subjets. This feature will be explored in more depth in a companion paper [1], which demonstrates the application of XCone for the examples of dijet resonances, Higgs decays to bottom quarks, and all-hadronic top pairs.

The possibility of using N-jettiness as a jet algorithm was already pointed out in ref. [5] and further explored in ref. [7]. Here, we more fully develop the idea of N-jettiness jets and present a concrete implementation of the XCone algorithm. As a global event shape, N-jettiness measures the degree to which the hadrons in the final state are aligned along N jet axes or the beam direction. It was originally introduced to veto additional jets in an event, providing a way to define and resum exclusive N-jet cross sections [5, 15, 16].[1] N-jettiness was later adapted to the jet shape N-subjettiness [6], which is an efficient measure to identify N-prong boosted hadronic objects such as top quarks, W/Z bosons, and Higgs bosons within a larger jet (see also [17]). By minimizing N-(sub)jettiness, one can directly identify N (sub)jet directions, and a fast algorithm to perform this minimization was presented in ref. [7]. N-jettiness jets have been used to resum the invariant mass of nearby jets [18], to make predictions for jet mass spectra [19, 20], for studying DIS and nuclear dynamics [21–26], and to define recoil-free jet observables [27]. As an N-jet resolution variable, N-jettiness has been utilized to combine perturbative calculations with parton showers in GENEVA [28], and very recently to define a powerful subtraction scheme for fixed-order calculations at next-to-next-to-leading order [29, 30].

As we will see, there is considerable flexibility in precisely how one defines N-jettiness, and several different N-jettiness measures yielding different jet regions have been considered before [5–7, 16, 19]. Here, as the XCone default, we propose a "conical geometric" measure that incorporates the insights from the different previous use cases. This measure is based on the dot product between particles and lightlike axes as in ref. [5] but incorporates an angular exponent β as in ref. [7], as well as a beam exponent γ for additional flexibility (see table 1 below). Crucially for the purposes of jet finding at the LHC, this measure yields (nearly) conical jets over a wide rapidity range, and the user can choose the desired jet radius R.

For most physics applications, we propose a default setting of $\beta = 2$ and $\gamma = 1$, which acts similarly to existing cone algorithms (see e.g. [31–34]) in that the resulting jet regions are (approximately) stable cones where the jet momenta and the jet axes align. The key

[1] The reader should be aware that there are two different definitions of "exclusive" which are both standard in their respective contexts. An exclusive N-jet *algorithm* is one that returns exactly N jets, regardless of what happens in the rest of the event. An exclusive N-jet *cross section* is the rate to produce exactly N jets, with a restriction on what happens in the rest of the event. XCone is an exclusive N-jet algorithm, but it can be used either to measure inclusive N-jet cross sections (if there are no restrictions made on unclustered particles) or an exclusive N-jet cross section (if there is a restriction, say, that $\mathcal{T}_N < \mathcal{T}_{\text{cut}}$).

JHEP11(2015)072

difference to algorithms like SISCone [34] is that XCone does not require a split/merge step. In particular, typical inclusive cone algorithms have an overlap parameter which determines whether two abutting stable cones should be joined or remain separate. By contrast, XCone only requires setting the jet radius R and the number of desired jets N, and the split/merge decision is determined dynamically through N-jettiness minimization. In a companion paper [1], we show examples of quasi-boosted kinematics that capitalize on this exclusive approach to cone jet finding.

There are interesting connections between N-jettiness minimization and previous work to define jets via cluster optimization [33, 35–43]. Stable cone finding is closely related to 1-jettiness minimization with $\beta = 2$ [33], and similar algorithms are relevant for a recently proposed "jet function"[2] optimization strategy [47–49]. One can even prove an exact equivalence between these algorithms when finding a single cone jet of fixed opening angle [50]. Finding the thrust axis [51] is related to 2-jettiness minimization with $\beta = 2$.[3] There is also an observable called triplicity [53] which is related to 3-jettiness. For a general N, k-means clustering [54] (with $k = N$) is a type of N-jettiness minimization, with $\beta = 2$ corresponding to traditional k-means and $\beta = 1$ corresponding to $R1$-k-means [55]. In all these cases, N-jettiness minimization is an infrared and collinear (IRC) safe procedure.

Because cluster optimization is a difficult computational problem, our practical XCone implementation will use recursive clustering algorithms [8, 56–59] to approximate N-jettiness minima. Roughly speaking, we run a generalized k_T clustering algorithm to determine IRC-safe seed jet axes as a starting point for an iterative one-pass minimization algorithm, in which N-jettiness is used to find the final jet axes and define the jet regions. Separating jet axes finding from jet region finding appeared previously in the context of recoil-free jets [27, 60], where a fixed radius cone was centered on winner-take-all axes [27, 61, 62] or broadening axes [7, 27]. XCone allows us to extend this strategy to N-jet events, with $\beta = 1$ yielding recoil-free jets and $\beta = 2$ yielding traditional cones where the jet axes and jet momenta are (nearly) aligned.

A key feature of the measures we consider, including the default XCone measure, is that N-jettiness can be decomposed into a direct sum of contributions from the jet and beam regions. When utilizing measures with this property, there exist active-parton factorization theorems for N-jettiness cross sections valid to all orders in α_s. Furthermore, the default XCone measure is linear in the particle momenta which greatly simplifies the calculation of the perturbative jet and soft functions needed to determine the N-jettiness cross section. Thus, the ingredients needed for higher-order logarithmic resummation or fixed-order calculations are simpler for jets defined with the XCone algorithm, in contrast for example to those defined with clustering algorithms like anti-k_T. We will discuss these factorization theorems in some detail for various choices of N-jettiness measures, including the XCone default.

[2]The name jet function in this context should not be confused with the more standard usage in the context of factorization of cross sections into hard, soft, and jet functions, e.g. [44–46]. Here our primary use of the name jet function will be in this factorization context, see section 5.

[3]Naively, one might think that spherocity [52] should be related to 2-jettiness with $\beta = 1$. However, minimizing this quantity does not give rise to the spherocity axis, but rather to kinked broadening axes [27].

JHEP11(2015)072

The remainder of this paper is organized as follows. In section 2, we review how to define an exclusive jet algorithm via minimizing N-jettiness. We then discuss a variety of N-jettiness measures in section 3, including the conical geometric measure that is the basis for XCone. In section 4, we discuss some details of our XCone implementation, in particular the choice of seed axes for finding a (local) N-jettiness minimum. In section 5, we discuss the factorization theorems for N-jettiness with various measures. This section is more theoretically technical than the others and may be skipped by readers not interested in this factorization. We conclude in section 6. The XCone algorithm is available through the NSubjettiness FastJet Contrib [63, 64] as of version 2.2.0.

2 N-jettiness as a jet algorithm

Given a set of normalized lightlike axes $n_A = \{1, \vec{n}_A\}$ with $\vec{n}_A^2 = 1$, N-jettiness is defined as[4]

$$\widetilde{\mathcal{T}}_N = \sum_i \min\left\{\rho_{\text{jet}}(p_i, n_1), \ldots, \rho_{\text{jet}}(p_i, n_N), \rho_{\text{beam}}(p_i)\right\} . \tag{2.1}$$

The sum runs over the four-momenta p_i of all particles that are considered as part of the hadronic final state and should take part in the jet clustering. The $\rho_{\text{jet}}(p_i, n_A)$ is a distance measure to the A-th axis n_A, and $\rho_{\text{beam}}(p_i)$ is a distance measure to the beam. Depending on the context, the beam measure can be separated into two beam regions with lightlike beam axes $n_{a,b}$ and (partonic) center-of-mass rapidity Y such that

$$\rho_{\text{beam}}(p_i) \Rightarrow \min\{\rho_{\text{beam}}(p_i, n_a, Y), \rho_{\text{beam}}(p_i, n_b, Y)\} . \tag{2.2}$$

This form will be relevant for the discussion in section 5.

For a given form of ρ_{jet} and ρ_{beam}, the minimum inside $\widetilde{\mathcal{T}}_N$ in eq. (2.1) partitions the particles i into N jet regions and an unclustered beam region. To use N-jettiness as a jet algorithm, one minimizes $\widetilde{\mathcal{T}}_N$ over all possible lightlike axes directions:

$$\mathcal{T}_N = \min_{n_1, n_2, \ldots, n_N} \widetilde{\mathcal{T}}_N . \tag{2.3}$$

The locations of the axes at the minimum define the centers of the jet regions. In previous applications, one uses a separate method to choose the N-jettiness axes n_A, e.g. from the N hardest jets found by some other jet algorithm. One then uses $\widetilde{\mathcal{T}}_N$ only for the jet partitioning (in which case there is no need to distinguish $\mathcal{T}_N \equiv \widetilde{\mathcal{T}}_N$). This use of $\mathcal{T}_N$ already provides a well-defined and IRC-safe way to define N exclusive jets. The additional overall minimization in eq. (2.3) over the axes n_A promotes $\mathcal{T}_N$ to a standalone exclusive jet algorithm. This axis minimization is nontrivial and we discuss our strategy to perform it in section 4.[5] Note that "minimization" can refer either to finding the global $\mathcal{T}_N$ minimum or using an IRC-safe procedure to find a local $\mathcal{T}_N$ minimum, either of which is suitable for the discussion below.

[4] Here we use a dimension-one definition as in refs. [16, 19] instead of the dimensionless τ_N used in ref. [5].

[5] One might also be able to dynamically determine the total rapidity Y or the beam axes $n_{a,b}$ through minimization, though that feature is currently not present in the XCone code.

JHEP11(2015)072

Name	$\rho_{\text{jet}}(p_i, n_A)$	$\rho_{\text{beam}}(p_i)$	$A \approx \pi R^2$?
Conical [7]	$p_{Ti}\left(\frac{R_{iA}}{R}\right)^{\beta}$	p_{Ti}	✓
General Conical	$p_{Ti}\, f(p_i)\left(\frac{R_{iA}}{R}\right)^{\beta}$	$p_{Ti}\, f(p_i)$	✓
Geometric [19]	$\frac{n_A \cdot p_i}{\rho_0}$	$m_{Ti}e^{-\lvert y_i\rvert}$	
Modified Geometric	$\frac{n_A \cdot p_i}{\rho_0}$	$\frac{m_{Ti}}{2\cosh y_i}$	
Geometric-R [19]	$\frac{n_A \cdot p_i}{\rho(R, y_A)}$	$m_{Ti}e^{-\lvert y_i\rvert}$	✓
Modified Geometric-R	$\frac{n_A \cdot p_i}{\rho_C(R, y_A)}$	$\frac{m_{Ti}}{2\cosh y_i}$	✓
Conical Geometric	$\frac{p_{Ti}}{(2\cosh y_i)^{\gamma-1}}\left(\frac{2\, n_A \cdot p_i}{n_{TA}\, p_{Ti}}\,\frac{1}{R^2}\right)^{\beta/2}$	$\frac{p_{Ti}}{(2\cosh y_i)^{\gamma-1}}$	✓
XCone Default ($\beta = 2, \gamma = 1$)	$\frac{2\cosh y_A}{R^2}\, n_A \cdot p_i$	p_{Ti}	✓
Recoil-Free Default ($\beta = 1, \gamma = 1$)	$\sqrt{\frac{2\cosh y_A}{R^2}\, p_{Ti}\, n_A \cdot p_i}$	p_{Ti}	✓
$\beta = 2$, $\gamma = 2$	$\frac{\cosh y_A}{\cosh y_i\, R^2}\, n_A \cdot p_i$	$\frac{p_{Ti}}{2\cosh y_i}$	✓

Table 1. N-jettiness measures studied in this paper. The conical geometric measure with $\beta = 2$ and $\gamma = 1$ is the suggested XCone default, giving stable cone jets (like the conical measure) through dot-product distances linear in p_i (like the geometric measures). The recoil-free variant with $\beta = 1$ centers the jet around its hardest cluster, making the jet regions less sensitive to soft contamination. In the conical geometric measure, $n_{TA} = 1/\cosh y_A$. In the (modified) geometric-R measures, $\rho_{(C)}(R, y_A)$ is a rapidity-dependent scale factor that yields jet areas of exactly πR^2 (though not conical jet boundaries). The checkmarks indicate measures that yield jets with active areas of $\approx \pi R^2$ for well-separated jets. These active areas are πR^2 to within $\lesssim 1\%$ over a wide rapidity range (see figure 4 below).

Any choice of measure together with the specific algorithm to minimize $\mathcal{T}_N$ defines an exclusive jet algorithm. In particular, $\mathcal{T}_N$ in eq. (2.1) always identifies N jet regions (and one beam region), regardless of how close the axes n_A might be to each other. When the axes are well separated, the boundary of the jet regions is determined through competition between ρ_{jet} and ρ_{beam}. When the axes are close together, the jet regions are determined by the competition between different ρ_{jet}.

To go from an exclusive jet algorithm to an exclusive *cone* jet algorithm (i.e. XCone), one wants the jet boundaries to approximate circles in the rapidity-azimuth plane, which can be achieved by an appropriate choice of jet and beam measures. In section 3, we study a variety of jet and beam measures which are summarized in table 1. This includes three new measures: the general conical measure in eq. (3.3) which yields exact cones for widely-separated jets; the modified geometric measure in eq. (3.10) whose jet measure is linear in particle momenta like the original geometric measure but exhibits smooth behavior at zero rapidity; and the recommended XCone default in eq. (3.18) which yields approximate cones and also features this linearity. By construction, the XCone default measure yield jets with approximately fixed active jet areas over a wide range of jet rapidities.

JHEP11(2015)072

In addition to partitioning the event into jet and beam regions, the returned value of $\mathcal{T}_N$ is a quality criterion that measures how well an event is characterized by N jets. The contribution to the $\mathcal{T}_N$ value from a given jet provides a measure of how collimated the jet is. For narrow jets (i.e. small effective jet radius), $\mathcal{T}_N$ is typically dominated by the contribution from the beam region. Thus, for LHC applications, one typically wants $\rho_{\text{beam}}(p_i)$ to be proportional to p_{Ti} (the transverse momentum of particle i) such that minimizing $\mathcal{T}_N$ results in the least unclustered p_T. Larger values of $\mathcal{T}_N$, and its beam contribution in particular, then indicate additional activity or hard jets in the event. An improved measure of jet quality can be obtained by examining the individual jet and beam contributions to $\mathcal{T}_N$, as in [16]:

$$\mathcal{T}_N = \mathcal{T}_N^{\text{beam}} + \mathcal{T}_N^{\text{jets}} = \mathcal{T}_N^{\text{beam}} + \sum_{A=1}^{N} \mathcal{T}_N^A \,. \tag{2.4}$$

Here, $\mathcal{T}_N^{\text{jets}}$ provides a global measure for assessing how collimated the jets are without contamination from the beam region, and one can obtain individual quality measures for each of the N jets by examining their individual numerical contributions $\mathcal{T}_N^A$ to the total N-jettiness. In section 5, we discuss some of the theoretical aspects involved in calculating $\mathcal{T}_N$ as well as the cross section that is fully differential in $\mathcal{T}_N^{\text{beam}}$ and the N observables $\mathcal{T}_N^A$.

Before discussing the specific measures, we want to make a general comment about underlying event and pileup, two effects that are known to impact jet reconstruction. While the *value* of $\mathcal{T}_N$ depends strongly on these effects, the jet regions found by minimizing $\mathcal{T}_N$ are no more sensitive to underlying event and pileup than traditional jet algorithms. The reason for this mismatch is that the beam contribution to the $\mathcal{T}_N$ value can get large contributions from these effects, but the change in $\mathcal{T}_N$ as the axes n_A are varied only depends on hadrons in the vicinity of the jet regions. This is particularly true for recoil-free measures, where the minimized axis direction is almost entirely insensitive to soft contamination [60]. For pileup specifically, the minimization in eq. (2.3) remains sensible even with negative energy particles, so one has the option of introducing negative energy ghosts as a way to implement area subtraction [9, 10, 65]. For isolated jets, one can derive a closed-form integral expression for the active jet area, which depends only mildly on the jet rapidity.

3 Choice of measure

As already mentioned, every choice of jet and beam measure defines some kind of N-jettiness jet algorithm. We now review previous measures in the literature en route to explaining the logic behind the new XCone default measure. Example jet regions found from some of these measures are shown in figures 1 and 2 for a boosted top event from the BOOST 2010 event sample [11]. In figure 3, we show a comparison between the XCone default and the anti-k_T algorithm [4]. While XCone and anti-k_T are very similar for widely separated jets as in figure 3(b), they behave quite differently when the jets are close together as in figure 3(a). A more extensive discussion and anti-k_T comparison can be found in the companion paper [1].

JHEP11(2015)072

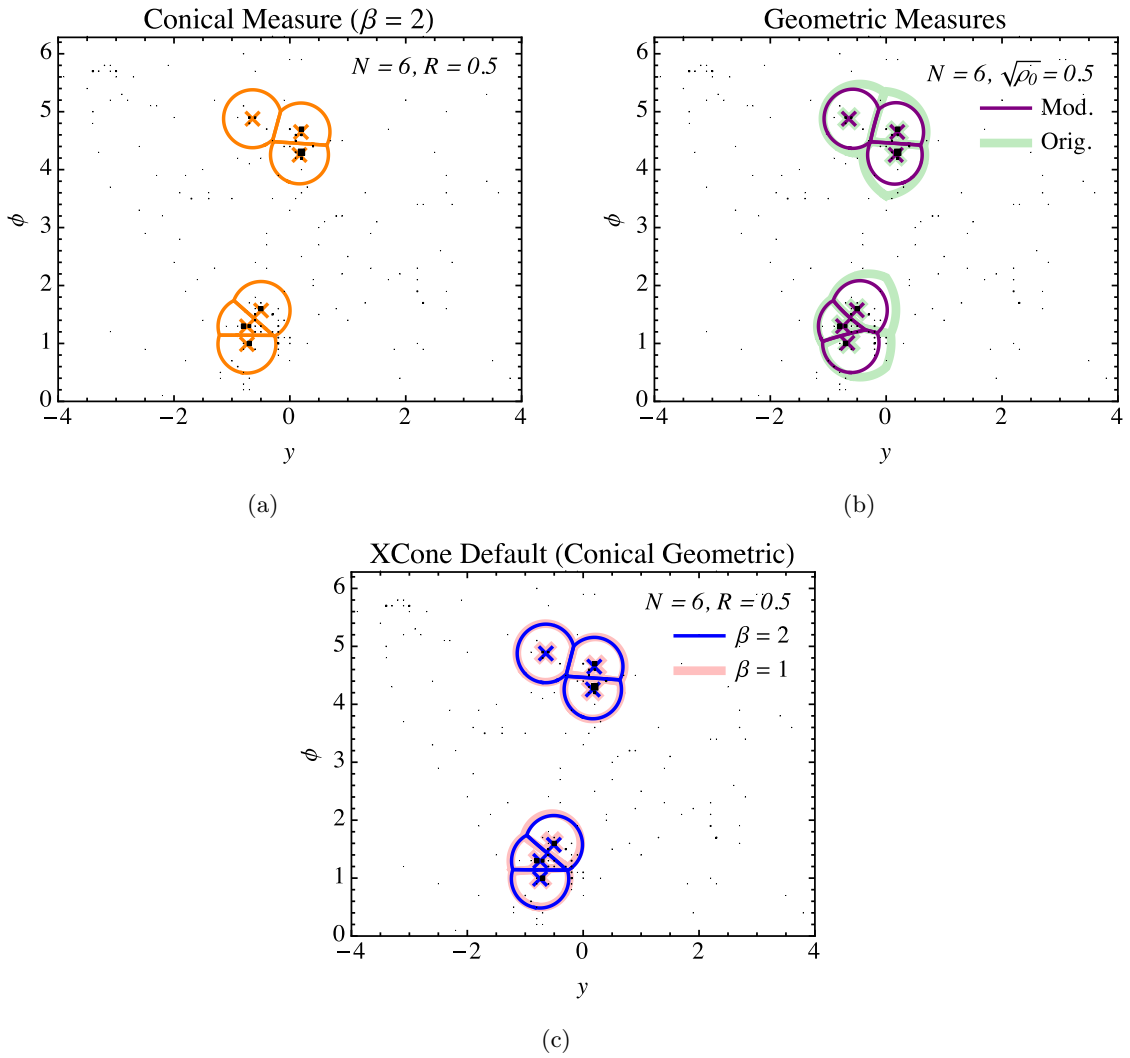

Figure 1. Jet regions found with various N-jettiness measures. This is a $t\bar{t}$ event from the BOOST 2010 event sample [11], and every measure has $N = 6$ and $R = 0.5$. (a) Conical measure with $\beta = 2$. (b) Original and modified geometric measures. (c) Conical geometric measure with $\beta = 2$ (XCone default) and $\beta = 1$ (recoil-free default). The conical and conical geometric measures yield (approximately) circular jets. For all measures, the overlap region between jets is automatically partitioned by nearest neighbor, as given by the jet measure.

3.1 The conical measure

The first conical N-jettiness measure was proposed in ref. [7]:[6]

Conical Measure

$$\rho_{\text{jet}}(p_i, n_A) = p_{Ti}\left(\frac{R_{iA}}{R}\right)^{\beta}, \qquad \rho_{\text{beam}}(p_i) = p_{Ti}\,, \tag{3.1}$$

[6]Strictly speaking, the measure in ref. [7] has an extra rapidity cut parameter.

JHEP11(2015)072

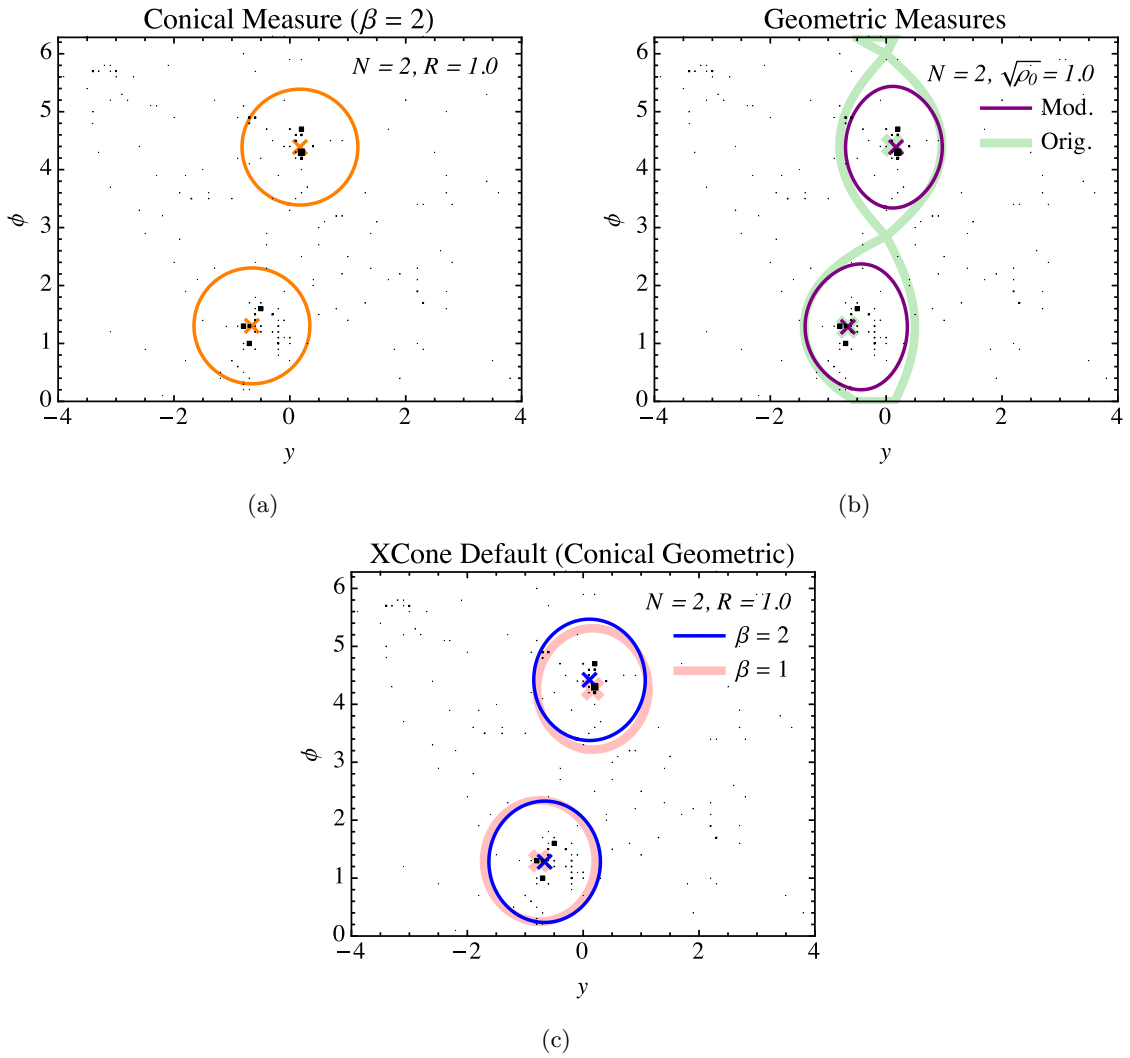

Figure 2. Same $t\bar{t}$ event as in figure 1, but for $N = 2$ and $R = 1.0$. (a) The conical measure yields exactly circular jet regions for widely-separated jets. (b) The geometric measure exhibits cusps at $y = 0$ which are smoothed out with the modified geometric measure. (c) The XCone default ($\beta = 2$) yields jets centered along the total jet momentum while the recoil-free default ($\beta = 1$) yields jets centered along the hardest cluster within the jet.

where

$$R_{iA} = \sqrt{(y_i - y_A)^2 + (\phi_i - \phi_A)^2} \tag{3.2}$$

is the distance between p_i and n_A in the rapidity-azimuth plane, and β is an angular weighting exponent. The parameter R acts like the jet radius in a cone algorithm, since particle i can only be clustered into jet A if $\rho_{\text{jet}}(p_i, n_A) < \rho_{\text{beam}}(p_i)$, which is equivalent to $R_{iA} < R$. Thus, the measure in eq. (3.1) yields jets that are exact circles with radius R in the rapidity-azimuth plane, as shown in figure 2(a), unless two jet axes are closer than R. When two or more axes are closer than R to each other, the jet regions are determined by Voronoi partitioning (i.e. nearest neighbor). This yields "clover jet" configurations as

JHEP11(2015)072

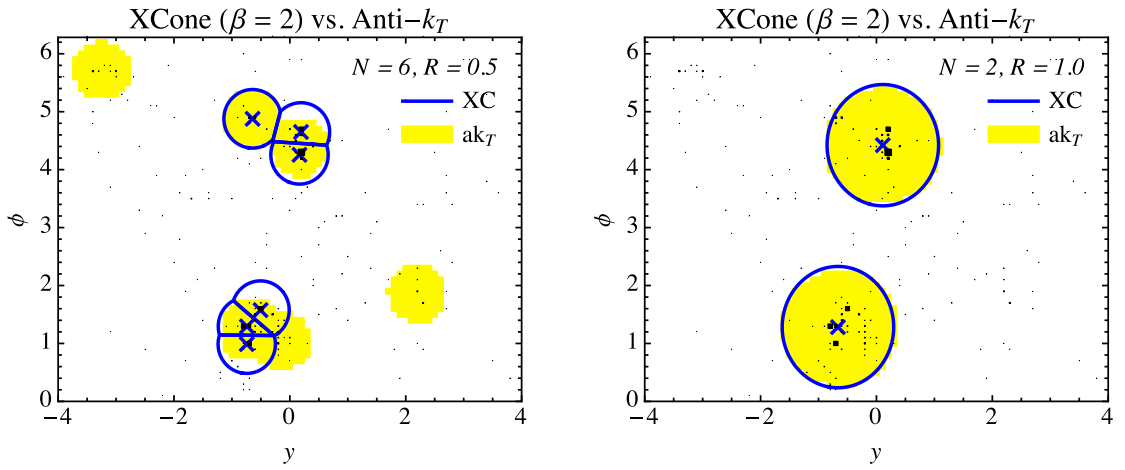

(a) (b)

Figure 3. Comparison between the XCone default ($\beta = 2$) and anti-k_T, using the same $t\bar{t}$ events as figures 1 and 2. (a) Unlike anti-k_T which merges jet regions closer in angle than $\approx R$, XCone allows such jet regions to remain split. (b) For widely-separated jets, XCone yields nearly identical jet regions to anti-k_T.

shown in figure 1(a).

For small R, $\mathcal{T}_N$ is dominated by the beam measure, which is just the unclustered p_T in an event. Thus, this measure typically finds the N jets with the largest p_T in an event. By adjusting the exponent β, the jet axis can be varied to point along the jet direction ($\beta = 2$, "mean") or along the hardest cluster inside a jet ($\beta = 1$, "median"), see also refs. [7, 27, 60].

Naively, the conical measure might seem to be the only measure yielding conical jets, since any change to the measure would affect the competition between ρ_{jet} and ρ_{beam} and change the style of the event partitioning. One can maintain conical jets, however, if one deforms eq. (3.1) via

General Conical Measure

$$\rho_{\text{jet}}(p_i, n_A) = p_{Ti}\, f(p_i) \left(\frac{R_{iA}}{R}\right)^{\beta}, \qquad \rho_{\text{beam}}(p_i) = p_{Ti}\, f(p_i)\,, \tag{3.3}$$

where $f(p_i)$ is any dimensionless function of the particle four-momentum. This measure still returns exactly conical jets with overlapping jets still having Voronoi partitioning, because the factor of $f(p_i)$ drops out when comparing ρ_{jet} to ρ_{beam} or when comparing two different ρ_{jet}. While the partitioning for given axes does not depend on $f(p_i)$, the $f(p_i)$ factor does play a role in determining the overall $\mathcal{T}_N$ minimum in eq. (2.3). So the final jets will have different axes depending on the choice of $f(p_i)$. We will exploit this possibility when defining the conical geometric measure in section 3.3.

JHEP11(2015)072

3.2 The geometric measure

A variety of N-jettiness measures were proposed and studied in refs. [16, 19]. For the purposes of defining a cone jet algorithm, the most promising choice is the geometric measure:

$$\boxed{\text{Geometric Measure}} \qquad \begin{aligned} \rho_{\text{jet}}(p_i, n_A) &= \frac{n_A \cdot p_i}{\rho_0}\,, \\ \rho_{\text{beam}}(p_i) &= \min\{n_a \cdot p_i,\, n_b \cdot p_i\}\,, \end{aligned} \tag{3.4}$$

where $n_{a,b} = \{1, 0, 0, \pm 1\}$ and the z-direction is the beam direction, such that

$$\min\{n_a \cdot p_i,\, n_b \cdot p_i\} = p_i^0 - |p_i^3| = m_{Ti} e^{-|y_i|}\,. \tag{3.5}$$

Here, $m_{Ti} = \sqrt{p_{Ti}^2 + m_i^2}$, y_i is the rapidity, and this is the form given in table 1.

The presence of the $n \cdot p_i$ dot product in the jet and beam measures is very natural from a theoretical perspective, since it makes the measure linear in both p_i and n. The linearity in the jet axes n_A implies that the total jet three-momentum is exactly aligned with the axis direction $\vec{n}_A$ (see section 4.2). The linearity in p_i implies simple factorization properties for $\mathcal{T}_N$ and also tends to make perturbative calculations much simpler (see e.g. refs. [16, 18, 19, 25, 30, 66]). For this reason all N-jettiness calculations so far which involve initial state hadrons have been based on measures linear in p_i, like the geometric measure.

Despite the presence of the dot product $n_A \cdot p_i$, the geometric measure actually behaves quite similarly to the conical measure.[7] To see this, note that the momenta p_i and lightlike axes n_A can be expressed as

$$p_i = \left\{m_{Ti} \cosh y_i,\, \vec{p}_{Ti},\, m_{Ti} \sinh y_i\right\}, \qquad p_{Ti} \equiv |\vec{p}_{Ti}|\,, \tag{3.6}$$

$$n_A = \left\{1,\, \vec{n}_{TA},\, \tanh y_A\right\}, \qquad n_{TA} \equiv |\vec{n}_{TA}| = \frac{1}{\cosh y_A}\,, \tag{3.7}$$

and their dot product is given by

$$\frac{n_A \cdot p_i}{n_{TA}\, p_{Ti}} = \frac{m_{Ti}}{p_{Ti}} \cosh(y_i - y_A) - \cos(\phi_i - \phi_A)\,. \tag{3.8}$$

In the limit of small angles and for massless particles we thus have

$$\rho_{\text{jet}}(p_i, n_A) = \frac{n_A \cdot p_i}{\rho_0} \approx \frac{p_{Ti}}{2\cosh y_A} \frac{R_{iA}^2}{\rho_0}\,. \tag{3.9}$$

Hence, the ρ_{jet} for the geometric measure acts similarly to the general conical measure in eq. (3.3) with $\beta = 2$ and $f(p_i) = 1/(2\cosh y_i)$, at least to the extent that $\cosh y_i \approx \cosh y_A$. This also shows that the parameter ρ_0 in the geometric measures controls the size of the jet regions with roughly $\rho_0 \simeq R^2$.

Since the geometric measure does not take the precise form of eq. (3.3), it yields football-like jets in the central region with cusps at $y = 0$, which get accentuated for larger

[7] In the context of recursive clustering algorithms, this dot-product form was also mentioned as an option in ref. [8].

JHEP11(2015)072

jets as shown by the green thick lines in figures 1(b) and 2(b). For overlapping jets, it produces similar clover jets due to the competition between the ρ_{jet} for different jets.

Although not as extreme as the jet shapes obtained with an invariant mass measure (see ref. [16]), these cusps in the jet boundaries are somewhat unnatural for experimental applications. Since the shape of the jet regions is determined by the competition between ρ_{jet} and ρ_{beam}, we can modify the geometric measure to yield more conical jets by introducing an explicit compensating factor of $f(p_i) = 1/(2\cosh y_i)$ in the beam measure:

Modified Geometric Measure

$$\begin{aligned} \rho_{\text{jet}}(p_i, n_A) &= \frac{n_A \cdot p_i}{\rho_0}\,, \\ \rho_{\text{beam}}(p_i) &= \frac{m_{Ti}}{2\cosh y_i}\,. \end{aligned} \tag{3.10}$$

With the approximations in eq. (3.9) and $\cosh y_i \approx \cosh y_A$ this modified measure is now approximately the same as eq. (3.3) with $\beta = 2$ and $f(p_i) = 1/(2\cosh y_i)$. Hence, it yields reasonably conical jets also in the central region, as shown by the purple lines in figures 1(b) and 2(b). This corresponds to only a slight modification of the geometric beam measure, since close to the beam axes, i.e. for large y_i, we have

$$\frac{m_{Ti}}{2\cosh y_i} \to m_{Ti}\, e^{-|y_i|}\,. \tag{3.11}$$

This implies that the modified geometric measure has very similar factorization properties as the geometric measure, which we will return to in section 5. The use of $1/(2\cosh y_i)$ to replace $e^{-|y_i|}$ is the same as the well-known distinction between using C-parameter [67, 68] and thrust [51] event shapes to describe the narrow dijet limit in e^+e^- collisions, see e.g. [69–72].

While we can roughly associate $\rho_0 \simeq R^2$, the jet area itself still differs from πR^2, especially for larger R and away from central jet rapidities. To enforce jets of a constant jet area, regardless of the jet rapidity and jet boundary, ref. [19] also introduced a geometric-R measure where the jet measure is rescaled by a rapidity-dependent factor to maintain πR^2 jet areas for widely-separated jets:

Geometric-R Measure

$$\begin{aligned} \rho_{\text{jet}}(p_i, n_A) &= \frac{1}{\rho(R, y_A)}\, n_A \cdot p_i\,, \\ \rho_{\text{beam}}(p_i) &= m_{Ti} e^{-|y_i|}\,. \end{aligned} \tag{3.12}$$

Here, $\rho(R, y_A)$ is given in terms of the the integral $I_0(\alpha, \beta)$ from [16] which determines the geometric jet area (for nonoverlapping jets) via the transcendental equation [20]

$$I_0\Big(\frac{a_+}{2\rho}, \frac{a_-}{2\rho}\Big) + I_0\Big(\frac{a_-}{2\rho}, \frac{a_+}{2\rho}\Big) = R^2\,, \qquad a_\pm = 1 \pm \tanh y_A\,. \tag{3.13}$$

Numerical results for ρ were given in ref. [19]. The same modifications as above lead to the modified geometric-R measure

Modified Geometric-R Measure

$$\begin{aligned} \rho_{\text{jet}}(p_i, n_A) &= \frac{1}{\rho_C(R, y_A)}\, n_A \cdot p_i\,, \\ \rho_{\text{beam}}(p_i) &= \frac{m_{Ti}}{2\cosh y_i}\,, \end{aligned} \tag{3.14}$$

JHEP11(2015)072

where $\rho_C(R, y_A)$ is different than in eq. (3.12) due to the difference in the beam measures.

In all of the above cases, the rapidity suppression in the beam measures at large rapidities makes $\mathcal{T}_N$ much less sensitive to the forward region. This means the $\mathcal{T}_N$ minimization effectively corresponds to minimizing a rapidity-weighted sum of unclustered p_T (i.e. the unclustered beam thrust [15] or "beam C-parameter" contribution). As a result, the algorithm will dominantly identify central jets over forward jets, which could have interesting applications, e.g. when one wants to avoid picking up forward jets from initial-state radiation. Corresponding forward-insensitive rapidity-weighted jet vetoes have been discussed recently in ref. [73].

3.3 The conical geometric measure

Combining the lessons of the conical and geometric measures, we now introduce the conical geometric measure which aims to combine their advantages. For a specific choice of parameters, this will be the XCone default measure.

Like the conical measure, we want a measure that returns (nearly) conical jets, and we also want a parameter β in the jet measure to adjust the behavior of the jet axes. Like the geometric measure, we want a measure that depends on the dot products between lightlike axes and particles, since that is the simplest distance to use in theoretical calculations, and can be made linear in the particle momentum (here by choosing $\beta = 2$). These requirements lead us to

Conical Geometric Measure

$$\rho_{\text{jet}}(p_i, n_A) = \frac{p_{Ti}}{(2\cosh y_i)^{\gamma-1}} \left(\frac{2n_A \cdot p_i}{n_{TA}\, p_{Ti}} \frac{1}{R^2}\right)^{\beta/2},$$
$$\rho_{\text{beam}}(p_i) = \frac{p_{Ti}}{(2\cosh y_i)^{\gamma-1}}, \tag{3.15}$$

where again $n_{TA} = 1/\cosh y_A$. In the jet measure, we recognize the last factor in parentheses as the approximate form for R_{iA} in eq. (3.8), which now yields jets that are very nearly conical. The β factor acts just like the β factor in the conical measure. For additional flexibility, we have chosen a common $f(p_i) = (2\cosh y_i)^{1-\gamma}$ in the beam and jet measures. This multiplicative factor affects the axes found by minimization, but not the beam and jet regions. It is parametrized by γ, such that for $\gamma = 1$ this reproduces the beam measure of the conical measure while for $\gamma = 2$ this is closely analogous to the beam measure of the modified geometric measures.

There is additional freedom in defining the conical geometric measure that we will not exploit in this paper. For example, we could multiply the jet or beam measures by any function of

$$\frac{m_{Ti}}{p_{Ti}}, \tag{3.16}$$

which would give slightly different behavior for massive hadrons. In the jet measure, we could multiply by any function of

$$\frac{\cosh y_i}{\cosh y_A}, \tag{3.17}$$

JHEP11(2015)072

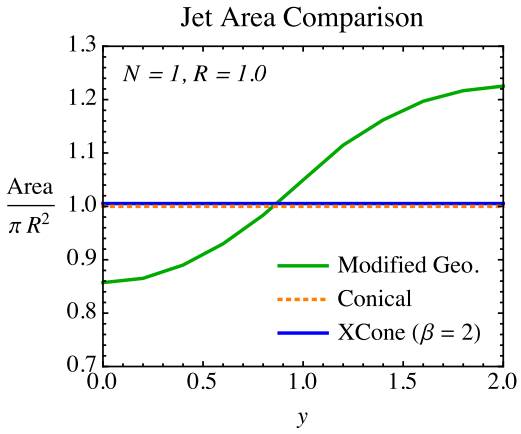

Figure 4. Comparison of the analytic jet areas for a single jet ($N = 1$). Unlike the modified geometric measure, the conical geometric measure (here shown for the XCone default of $\beta = 2$) has uniform jet areas as a function of rapidity. For $R \lesssim 1.0$, this area is within 1% of πR^2 from the conical measure.

since this quantity is nearly one for narrow jets. For example, the modified geometric measure is reproduced exactly by taking $\beta = \gamma = 2$ and in addition multiplying the beam and jet measures by m_{Ti}/p_{Ti} and $\cosh y_i / \cosh y_A$, respectively. These choices are somewhat analogous to the choice of recombination schemes in recursive jet algorithms, since they are irrelevant for infinitely narrow cones and massless inputs. That said, for $\beta = 2$, $\gamma = 2$ the factor of $\cosh y_A / \cosh y_i$ that appears in the conical geometric measure relative to the (modified) geometric measure ensures that the jet area is very close to πR^2 even for relatively forward jets, as shown in figure 4.

3.4 The XCone default measure

For LHC applications, our recommended XCone default is the conical geometric measure with $\beta = 2$ and $\gamma = 1$:

XCone Default Measure ($\beta = 2$)

$$\rho_{\text{jet}}(p_i, n_A) = \frac{2\cosh y_A}{R^2}\, n_A \cdot p_i \,, \qquad \rho_{\text{beam}}(p_i) = p_{Ti} \,. \tag{3.18}$$

By choosing $\gamma = 1$, the beam measure is the same as the conical measure, so minimizing $\mathcal{T}_N$ minimizes the unclustered p_T. By choosing $\beta = 2$, the jet axis (approximately) aligns with the total three-momentum of the jet, as is typical for traditional stable cone algorithms. Note that the jet measure is linear in p_i, as desired for theoretical calculations. In figure 4 we show that the active area of XCone jets is very nearly πR^2 for well-separated jets, see also ref. [1].

Alternatively, in cases where recoil-sensitivity [74–77] is an issue (such as in high pileup

JHEP11(2015)072

environments [60]) we can use $\beta = 1$ and $\gamma = 1$:

Recoil-Free Default Measure ($\beta = 1$)

$$\rho_{\text{jet}}(p_i, n_A) = \sqrt{\frac{2\cosh y_A}{R^2}\, p_{Ti}\, n_A \cdot p_i}\,,$$
$$\rho_{\text{beam}}(p_i) = p_{Ti}\,. \tag{3.19}$$

Here, the jet center aligns approximately along the broadening axis of the jet [7, 27], which is the axis that minimizes the summed transverse momentum relative to it. This is similar to finding the "median" jet energy and the jet axis tends to point along the most energetic cluster within a given jet. Again, the jet area is approximately πR^2.

These XCone default measures are the basis for our LHC case studies in the companion paper [1], where we find that both $\beta = 2$ and $\beta = 1$ give comparable results for jet reconstruction (in the absence of jet contamination). The jet regions for XCone default are shown in figures 1(c) and 2(c). With a single energetic cluster inside a jet, the difference between $\beta = 2$ and $\beta = 1$ is very small (again in the absence of jet contamination), analogous to the way that the mean and median of a peaked distribution are very similar. This is shown in figure 1(c). When a jet has substructure, the "mean" ($\beta = 2$) and "median" ($\beta = 1$) axes are offset, as shown in figure 2(c) for the same event with $N = 2$. One can also see that for larger jet radius, the jet regions are slightly elongated along the azimuthal direction compared to the rapidity direction. This arises because of the trigonometric functions in eq. (3.8). In ref. [1] it is mentioned that this deformation from exact circles yields slightly improved performance when reconstructing invariant-mass peaks.

4 Details of the XCone algorithm

For a given N-jettiness measure entering in eq. (2.1), we need to implement the minimization procedure in eq. (2.3) to determine the jet axes n_A. In general, the only guaranteed method to find the global minimum of $\mathcal{T}_N$ is to test by brute force all possible partitions of the final-state particles into N jet regions and one beam region. Since this is computationally prohibitive, our aim is to find good approximations of the global minimum by relying on methods that strictly speaking only find local minima of $\mathcal{T}_N$. Even if the algorithm does not find a guaranteed global $\mathcal{T}_N$ minimum, as long as all steps are fully specified and IRC safe, it still represents a well-defined exclusive cone algorithm which retains the key features of the N-jettiness partitioning according to the specified jet and beam measures.

Throughout this section, we restrict ourselves to the case $\gamma = 1$, which is currently implemented in the XCone code and is also used by the default measures.

4.1 One-pass minimization

For the conical measure in eq. (3.1), ref. [7] introduced a modification of Lloyd's method [54] that finds a local minimum of $\mathcal{T}_N$ for $1 < \beta < 3$. We can adopt a similar strategy for more general measures.

Our minimization algorithm proceeds as follows, with more details given below:

1) *Find seed axes:* determine a set of suitable IRC-safe initial axes n_A.

JHEP11(2015)072

2) *Assignment:* for fixed axes n_A, assign particles to jet and beam regions via $\mathcal{T}_N$ partitioning.

3) *Update axes:* for fixed partitioning, update axes n_A via $\mathcal{T}_N$ minimization.

4) If axes have converged then stop, otherwise go back to step 2).

To be IRC safe, this procedure must be fully deterministic. We therefore always perform a one-pass minimization, i.e., the above algorithm is repeated precisely once per event without any stochastic elements (such as random variations in the seed axes). The procedure to determine the seed axes in step 1) is deterministic and IRC safe, as described in section 4.3. The seed axes are then iteratively improved to a local minimum of $\mathcal{T}_N$ in steps 2) and 3).

In the assignment step 2), the final-state particles are assigned to one of the N jet regions or to the beam region via the $\mathcal{T}_N$ partitioning in eq. (2.1) for the current set of fixed trial axes n_A. This step can be easily implemented for any choice of measure as it only depends on the competition between the jet measures $\rho_{\text{jet}}(n_A, p_i)$ for fixed n_A and the beam measure $\rho_{\text{beam}}(p_i)$, so we do not need to discuss it further.

In the update step 3), the axes n_A are improved to minimize the contribution to the $\mathcal{T}_N$ value within each jet region, keeping the jet constituents determined by the partitioning in the previous assignment step fixed. Different update steps are needed for different measures, since there is no general procedure to find the axes n_A that minimize $\sum_i \rho_{\text{jet}}(n_A, p_i)$.[8] Once an appropriate update step is found, the assignment and update steps can be iterated until the axes converge to within some specified accuracy. In section 4.2, we describe a general update step that works well for the measures studied in this paper.

As discussed in ref. [7], these one-pass minimization procedures are quite effective for N-subjettiness, often converging to the global minimum. There are additional complications, however, for N-jettiness. The reason is that N-jettiness has a beam region, and particles in the bulk of the beam region are insensitive to small changes to the location of the jet axes n_A. Even minimization routines that try to go "uphill" to escape local minima may never find the optimal jet axes. Given that $\mathcal{T}_N$ corresponds roughly to the unclustered p_T in an event (for $\gamma = 1$), failing to find a decent $\mathcal{T}_N$ minimum means that one will identify too many soft jets. Therefore, for XCone to be a practical jet algorithm, one has to find a good set of seed axes for one-pass minimization. In section 4.3, we show how to find such seed axes by utilizing recursive clustering algorithms.

Another possibility to further improve the $\mathcal{T}_N$ minimization is by running the above (or any other) exclusive jet algorithm to find $N+n$ jets. Starting from these, one can then perform the remaining partitioning into N jets by explicitly testing all possible combinatorial options to find the best minimum. This option is available in the XCone code, though not recommended by default for reasons of speed. One advantage of this strategy is that it reduces to the exact $\mathcal{T}_N$ minimization for up to $N+n$ final-state particles. This makes it convenient for fixed-order calculations up to N^{n}LO, where the one-pass minimization with seed axes could induce rather complicated boundaries in the phase-space integrations.

[8] Even if one does find such a procedure, one has to check on a case-by-case basis whether the assignment/update iteration actually converges when using it. Some pathological cases were discussed in ref. [7].

JHEP11(2015)072

4.2 Update step for general measures

We now construct a general update step that converges to a local minimum of $\rho_{\text{jet}}(n_A, p_i)$ for a fixed set of jet constituents with momenta p_i. This approach works for a wide variety of jet measures, including the XCone defaults.

To motivate our general procedure, we start with the special case of the (modified) geometric measure, where finding a local minimum of ρ_{jet} is particularly straightforward. Within a given jet region A, we want to find the axis n_A that minimizes

$$\sum_{i \in A} n_A \cdot p_i = n_A \cdot \left(\sum_{i \in A} p_i \right) \equiv n_A \cdot p_A \,, \tag{4.1}$$

where $p_A = \sum_{i \in A} p_i$ is the total four-momentum of all jet constituents. Introducing a Lagrange multiplier λ (as in [50]), the quantity

$$n_A \cdot p_A + \lambda(\vec{n}_A^2 - 1) \tag{4.2}$$

is minimized for

$$n_A = \left\{ 1, \frac{\vec{p}_A}{|\vec{p}_A|} \right\} \qquad \text{with} \qquad \vec{p}_A = \sum_{i \in A} \vec{p}_i \,, \tag{4.3}$$

such that the jet axis $\vec{n}_A$ exactly aligns with the total three-momentum of the jet. Thus, minimizing the modified geometric measure is equivalent to finding N mutually stable (Voronoi-bounded) cones. In the same way, any measure of the form

$$\rho_{\text{jet}}(n_A, p_i) = n_A \cdot p_i \, f(p_i) \tag{4.4}$$

will be minimized by

$$n_A = \left\{ 1, \frac{\vec{q}_A}{|\vec{q}_A|} \right\} \qquad \text{with} \qquad \vec{q}_A = \sum_{i \in A} \vec{p}_i \, f(p_i), \tag{4.5}$$

where $\vec{q}_A$ is the effective total three-vector of the f-weighted jet constituents. For these cases, one-pass minimization will terminate in a finite number of assignment/update steps.

The conical geometric measure does not take the form of eq. (4.4), but rather takes the more general form

$$\rho_{\text{jet}}(n_A, p_i) = n_A \cdot p_i \, g(p_i, n_A), \tag{4.6}$$

where the jet measure has nonlinear dependence on n_A. This means that the jet axis and the jet three-momentum do not in general align. For the XCone default measure in particular, the extra factor of $\cosh y_A$ in the jet measure means that there is an offset between the axis and the momentum proportional to the jet mass. Thus, we cannot directly use the above stable-cone finding logic to minimize ρ_{jet}. Instead, as in ref. [7], we can define an update step based on the previous n_A value:[9]

$$n_A^{\text{new}} = \left\{ 1, \frac{\vec{q}_A}{|\vec{q}_A|} \right\} \qquad \text{with} \qquad \vec{q}_A = \sum_{i \in A} \vec{p}_i \, g(p_i, n_A^{\text{old}}). \tag{4.7}$$

[9] For practical purposes, it is sometimes necessary to include an "effective mass" term by changing $n_A \cdot p_i \to n_A \cdot p_i + \epsilon$ with small ϵ to avoid potential divide-by-zero errors.

JHEP11(2015)072

As long as the dependence on n_A is mild enough (roughly $1 \leq \beta < 3$ for the conical geometric measure), this procedure will converge within a desired accuracy in a reasonable number of assignment/update iterations, and we adopt this strategy for the XCone default measures. (In practice, due to the presence of local minima, the one-pass minimization may converge to a higher value of $\mathcal{T}_N$ than the original seed axes value. For this reason, we always return the smallest $\mathcal{T}_N$ value and associated axes seen among all update steps.)

4.3 Seed axes for one-pass minimization

Recursive clustering algorithms are particularly effective to find seed axes for one-pass minimization. When run in exclusive mode, a recursive clustering algorithm returns exactly N jets which can then be interpreted as N lightlike seed axes. In fact, the axes are often so good in practice that the iterative improvement step is unnecessary. One could even imagine a more general strategy that separates jet axis finding (here using recursive clustering) from jet region finding (here using N-jettiness partitions), and we plan to pursue this possibility in future work. Unlike generic cluster optimization, recursive clustering algorithms are computationally efficient, and this efficiency is inherited by our XCone implementation (at the expense of only guaranteeing a local $\mathcal{T}_N$ minimum).

For the conical geometric measures with $\gamma = 1$, including the XCone defaults, good seed axes can be found by running the generalized k_T clustering algorithm with a generalized E_t recombination scheme. The generalized k_T clustering measure [4, 63] is parametrized by an exponent p and a jet radius R:

$$d_{ij} = \min\left(p_{Ti}^{2p}, p_{Tj}^{2p}\right)\frac{R_{ij}^2}{R^2}, \qquad d_{iB} = p_{Ti}^{2p}, \tag{4.8}$$

where $p = 1$ is the k_T algorithm [8, 56] and $p = 0$ is the Cambridge/Aachen algorithm [57–59]. The generalized E_t recombination scheme is parametrized by an energy-weighting power δ, such that one obtains a massless recombined four-momentum p_r given by

$$p_{Tr} = p_{Ti} + p_{Tj}, \qquad \phi_r = \frac{p_{Ti}^{\delta}\phi_i + p_{Tj}^{\delta}\phi_j}{p_{Ti}^{\delta} + p_{Tj}^{\delta}}, \qquad \eta_r = \frac{p_{Ti}^{\delta}\eta_i + p_{Tj}^{\delta}\eta_j}{p_{Ti}^{\delta} + p_{Tj}^{\delta}}, \tag{4.9}$$

where $\delta = 1$ is the original E_t scheme, $\delta = 2$ is the E_t^2 scheme [8, 78], and $\delta = \infty$ is the winner-take-all scheme [27, 61, 62].

For finding seed axes, the recommended parameters for $0 < \beta < 2$ are

$$p \simeq \frac{1}{\beta}, \qquad \delta \simeq \frac{1}{\beta - 1}, \tag{4.10}$$

with matching radius parameter R. To understand this heuristic choice, consider starting with a final state of $N + 1$ particles and running one iteration of exclusive generalized k_T to find N axes. For this procedure to give good seed axes for $\mathcal{T}_N$ minimization, we want to choose the values of p and δ that match the behavior of the N-jettiness metric as closely as possible. Essentially, we want d_{iB} to match the beam measure ρ_{beam}, d_{ij} to match the jet measure ρ_{jet}, and the recombination scheme to appropriately place the merged axis in the desired location.

JHEP11(2015)072

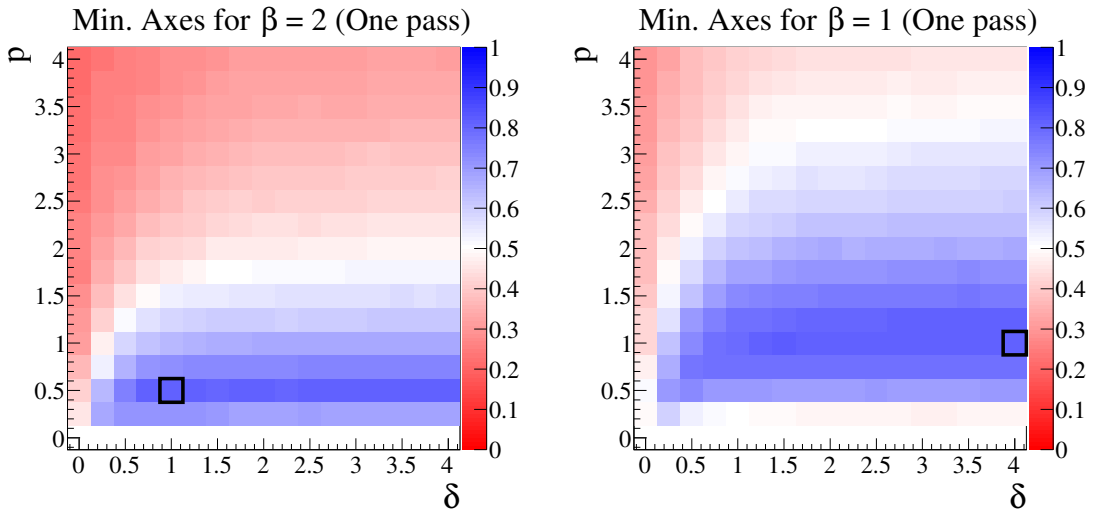

(a) (b)

Figure 5. Fraction of events where all XCone jets from one-pass minimization starting from generalized k_T jet axes as seeds align with the axes from global $\mathcal{T}_N$ minimization. This is for the BOOST 2010 top sample (Herwig 6.5, $p_T \in [500, 600]$ GeV) [11], using the conical geometric measure with $N = 6$ and $R = 0.5$. (a) The XCone default ($\beta = 2$). (b) The recoil-free default ($\beta = 1$). Here, p and δ parametrize the generalized k_T metric and recombination scheme, respectively. The black boxes indicate the preferred values of p and δ from the heuristic choice in eq. (4.10) (with $\delta = 4$ indicating $\delta \to \infty$).

We perform this heuristic analysis for the conical measure, which is a bit easier to understand than the conical geometric measure, though the same conclusions hold. To match the conical beam measure, generalized k_T with $p \geq 0$ already gives the right behavior, since the softest particle farther than R from any other particle is merged with the beam.[10]

To match the conical jet measure, we want d_{ij} to depend on the combination $p_{Ti} R_{ij}^{\beta}$, which is achieved for

$$p = \frac{1}{\beta}\,. \tag{4.11}$$

To match the conical axis behavior, we have to know which axis minimizes the $\mathcal{T}_N$ value for a jet region consisting of two particles. Labeling the two particles 1 and 2 and simplifying to one dimension ϕ without loss of generality, we have

$$\mathcal{T}_N \sim p_{T1} |\phi_1 - \phi_A|^{\beta} + p_{T2} |\phi_2 - \phi_A|^{\beta}\,, \tag{4.12}$$

where ϕ_A is the location of the axis. Solving $\mathrm{d}\mathcal{T}_N/\mathrm{d}\phi_A = 0$ to find the location of the minimum, we find

$$\phi_A = \frac{p_{T1}^{\delta}\phi_1 + p_{T2}^{\delta}\phi_2}{p_{T1}^{\delta} + p_{T2}^{\delta}}, \qquad \delta = \frac{1}{\beta - 1}\,, \tag{4.13}$$

which is exactly the generalized E_t recombination scheme. This is the logic behind the heuristic choice in eq. (4.10).

[10] In principle, it is possible to also handle the $\gamma \neq 1$ case by further modifications of eq. (4.8) (such as those proposed in ref. [79]), but we have not attempted that for the present XCone implementation.

JHEP11(2015)072

(a)

($\beta = 2$)	Seed axes	One-pass min
Jets	0.95	0.96
Events (≥ 4)	0.99	0.99
Events (≥ 5)	0.92	0.93
Events (6)	0.78	0.81

(b)

($\beta = 1$)	Seed axes	One-pass min
Jets	0.95	0.97
Events (≥ 4)	0.99	0.99
Events (≥ 5)	0.97	0.98
Events (6)	0.72	0.81

Table 2. Fraction of XCone jets that are aligned with the "true" minimum from global $\mathcal{T}_N$ minimization using only the seed axes from generalized k_T jets and after one-pass minimization for (a) $\beta = 2$ and (b) $\beta = 1$. Also shown are the fraction of all events with 4 or more, 5 or more, and all 6 jets aligned with the global minimum.

To explicitly validate the choice in eq. (4.10), we consider a sample of boosted top quarks from the BOOST 2010 report [11], using $N = 6$ and $R = 0.5$. A key feature of this boosted top sample is the presence of initial-state radiation, which generates an additional seventh hard jet in the event, providing a nontrivial test scenario. We first determine by brute force the global $\mathcal{T}_N$ minimum, as best as we can, by performing one-pass minimization on a wide range of seed axes. Next, we perform the one-pass minimization with the generalized k_T jets as seed axes for a range of p and δ values. For each p and δ, we then count the fraction of events that have all $N = 6$ XCone jet axes within $\Delta R < 0.1$ of the axes found from global $\mathcal{T}_N$ minimization. The results are shown in figure 5, which shows that the choice in eq. (4.10), shown by the black boxes, does give the best performance. We also observe that a wide range of δ values give similar results, while the choice of p is more relevant, especially for $\beta = 2$.

The fraction of aligned XCone jets, as well as the fraction of events where ≥ 4, ≥ 5, and all 6 XCone jets are aligned with the global minimum, both before and after one-pass minimization, are shown in tables 1(a) and 1(b). Even without one-pass minimization, i.e. using the seed axes only, 95% of the individual jets are closely aligned with the global $\mathcal{T}_N$ minimization for both $\beta = 2$ and $\beta = 1$. This suggests that finding local $\mathcal{T}_N$ minima from generalized k_T seed axes is a robust procedure that often results in a global $\mathcal{T}_N$ minimum.

The presence of additional hard jets from initial-state radiation can of course confuse $N = 6$ jet finding, leading to a roughly 70-80% success rate for correctly identifying all 6 jets originating from the top decays. It is also not obvious that $\mathcal{T}_N$ minimization will necessarily always yield the best boosted top reconstruction, and it might well be that "failed" $\mathcal{T}_N$ minima are still useful for physics analyses. For a detailed study of the phenomenological aspects we refer to ref. [1], which also explores an $N = 2 \times 3$ strategy for this final state.

JHEP11(2015)072

5 N-jettiness factorization with various measures

A key attribute that originally motivated the use of N-jettiness is its factorization properties in the limit $\widetilde{\mathcal{T}}_N \to 0$ [5], which greatly simplifies calculations of the corresponding exclusive jet cross sections. The original N-jettiness factorization theorem was derived for active-parton cross sections[11] using techniques from Soft-Collinear Effective Theory (SCET) [83–87], which we also make use of here. So far, these properties have only been fully studied for situations where the measure is linear in a component of the particle momenta [5, 15, 16, 21], which simplifies the objects appearing in the factorization theorem. The examples studied thus far include the geometric and geometric-R measures in table 1.

In this section, we derive the factorization properties for more general measures. We will start with a generic analysis and eventually focus on $\beta = 2$ jet measures. We investigate the impact of the choice of jet axes and different beam measures. We also explain how transverse momentum conservation restricts the range of jet observables that can be calculated using the simplest version of the N-jettiness factorization theorem.

5.1 Separating into jet and beam regions

Due to the linear sum over particles i in eq. (2.1), N-jettiness can be obtained by adding up distinct contributions from the beam and N jet regions r

$$\widetilde{\mathcal{T}}_N = \sum_r \widetilde{\mathcal{T}}_N^r = \widetilde{\mathcal{T}}_N^a + \widetilde{\mathcal{T}}_N^b + \widetilde{\mathcal{T}}_N^1 + \cdots + \widetilde{\mathcal{T}}_N^N \,. \tag{5.1}$$

If only a single measurement is made on the beams as in eq. (2.1), we can simply use $\widetilde{\mathcal{T}}_N^a + \widetilde{\mathcal{T}}_N^b = \widetilde{\mathcal{T}}_N^{\text{beam}}$ here. Thus the N-jettiness cross section is obtained from the more fundamental cross section which is fully differential in the $\widetilde{\mathcal{T}}_N^i$ for each region,

$$\frac{\mathrm{d}\sigma(X_N)}{\mathrm{d}\widetilde{\mathcal{T}}_N} = \int\biggl[\prod_r \mathrm{d}\widetilde{\mathcal{T}}_N^r\biggr]\delta\Bigl(\widetilde{\mathcal{T}}_N - \sum_r \widetilde{\mathcal{T}}_N^r\Bigr)\frac{\mathrm{d}\sigma(X_N)}{\mathrm{d}\widetilde{\mathcal{T}}_N^a \mathrm{d}\widetilde{\mathcal{T}}_N^b \mathrm{d}\widetilde{\mathcal{T}}_N^1 \cdots \mathrm{d}\widetilde{\mathcal{T}}_N^N}\,, \tag{5.2}$$

where the products and sum run over $r = a, b, 1, \ldots, N$. Here X_N denotes a set of measurements made on the N signal jets and on other final-state particles like electroweak bosons or nonhadronic decay products which we write as follows

$$\frac{\mathrm{d}\sigma(X_N)}{\mathrm{d}\widetilde{\mathcal{T}}_N^a \mathrm{d}\widetilde{\mathcal{T}}_N^b \mathrm{d}\widetilde{\mathcal{T}}_N^1 \cdots \mathrm{d}\widetilde{\mathcal{T}}_N^N} = \int \mathrm{d}\Phi_N \sum_\kappa s_\kappa \frac{\mathrm{d}\sigma_\kappa(\Phi_N)}{\mathrm{d}\widetilde{\mathcal{T}}_N^a \mathrm{d}\widetilde{\mathcal{T}}_N^b \mathrm{d}\widetilde{\mathcal{T}}_N^1 \cdots \mathrm{d}\widetilde{\mathcal{T}}_N^N} X_N(\Phi_N)\,. \tag{5.3}$$

Here, the sum over κ runs over all relevant partonic channels $\kappa = \{\kappa_a, \kappa_b; \kappa_1, \ldots, \kappa_N\}$ for the underlying $2 \to N$ process (or $2 \to N + L$ where L denotes additional non-strongly-interacting final states). The s_κ is the appropriate factor to take care of symmetry factors

[11] We only consider factorization for active-parton cross sections, initiated by incoming quarks or gluons, in order to avoid the complications associated with the spectator partons present for incoming hadrons, such as Glauber effects [80–82]. When using these active-parton factorization theorems, it is nevertheless often assumed that the initial-state quarks and gluons are determined by standard parton distributions. For the N-jettiness observables, Glauber effects have not been fully treated in the literature.

JHEP11(2015)072

and flavor and spin averaging for each partonic channel. The $\mathrm{d}\Phi_N$ corresponds to the complete phase-space measure of the Born process with massless partons,

$$\int \mathrm{d}\Phi_N \equiv \frac{1}{2E_{\mathrm{cm}}^2} \int \frac{\mathrm{d}x_a}{x_a} \frac{\mathrm{d}x_b}{x_b} \int \mathrm{d}\Phi_N(q_a + q_b; q_1, \ldots, q_N, q) \frac{\mathrm{d}q^2}{2\pi} \mathrm{d}\Phi_L(q)\,, \tag{5.4}$$

where $\mathrm{d}\Phi_N(\ldots)$ on the right-hand side denotes the standard Lorentz-invariant N-particle phase space, and $\mathrm{d}\Phi_L(q)$ the remaining nonhadronic phase space with total momentum q. The variables appearing here and the restrictions we impose on the measurement function $X_N(\Phi_N)$ will be described further below.

Now consider $\widetilde{\mathcal{T}}_N$ in the exclusive N-jet limit $\widetilde{\mathcal{T}}_N \to 0$. Since we are interested in the simplest form of the factorization theorem, we assume that the jets are well separated from each other and from the beams, with no strong hierarchies in the jet p_Ts. We also assume that if we are computing the cross section differential in $\widetilde{\mathcal{T}}_N^r$, we have parametrically $\widetilde{\mathcal{T}}_N^r \sim \widetilde{\mathcal{T}}_N^{r'}$.[12] For definiteness we assume that the components in the decomposition in eq. (5.5) below scale homogeneously, which will indeed be the case if the only N-jettiness that we measure is the total $\widetilde{\mathcal{T}}_N$. In the exclusive N-jet limit, the final state consists of only soft radiation and so-called n_r-collinear energetic radiation which is collinear to one of the jet or beam directions n_r. Here, the key property of N-jettiness is the presence of the minimum in its definition, which leads to a linear decomposition for both $\widetilde{\mathcal{T}}_N$ and $\widetilde{\mathcal{T}}_N^r$. Namely, they can be decomposed as a sum of contributions coming from each of these types of emissions,

$$\widetilde{\mathcal{T}}_N = \widetilde{\mathcal{T}}_N^{[n_a]} + \widetilde{\mathcal{T}}_N^{[n_b]} + \widetilde{\mathcal{T}}_N^{[n_1]} + \ldots + \widetilde{\mathcal{T}}_N^{[n_N]} + \widetilde{\mathcal{T}}_N^{[\mathrm{soft}]}\,, \qquad \widetilde{\mathcal{T}}_N^r = \widetilde{\mathcal{T}}_N^{[n_r]} + \widetilde{\mathcal{T}}_N^{r[\mathrm{soft}]}\,, \tag{5.5}$$

where the $[n]$ superscripts refer to the contribution from emissions collinear to the n-direction, and [soft] to soft emissions. For definiteness, we let

$$n_a = (1, \hat{z})\,, \qquad n_b = (1, -\hat{z})\,, \tag{5.6}$$

where $\hat{z}$ is the physical beam direction.

Equation (5.5) encodes the fact that for all of the measures in table 1, the n_r-collinear emissions only contribute to the measurement in the r-th region, while the soft radiation contributes to all regions and can itself be decomposed as in eq. (5.1). This linearity is the key property that allows deriving a factorization theorem which decomposes the exclusive N-jet cross section into a product of functions for each type of radiation. The basic form of the N-jettiness factorization theorem is [5]

$$\frac{\mathrm{d}\sigma_\kappa(\Phi_N)}{\mathrm{d}\widetilde{\mathcal{T}}_N} = \mathrm{tr}\; \widehat{H}_N^\kappa \otimes B_{\kappa_a} \otimes B_{\kappa_b} \otimes J_{\kappa_1} \otimes \ldots \otimes J_{\kappa_N} \otimes \widehat{S}_N^\kappa\,. \tag{5.7}$$

Here, $\widehat{H}_N^\kappa$ is a hard function, B_{κ_a,κ_b} are beam functions, J_{κ_A} is a jet function for the A-th jet region, and $\widehat{S}_N^\kappa$ is a soft function. A description of the variables these objects depend on will be given below. We note immediately that $\widehat{H}_N^\kappa$ depends directly on the full partonic

[12] This last assumption avoids the appearance of large nonglobal logarithms, $\ln(\widetilde{\mathcal{T}}_N^r/\widetilde{\mathcal{T}}_N^{r'})$. These logarithms will not appear when considering the cross section differential only in the total $\widetilde{\mathcal{T}}_N$.

JHEP11(2015)072

channel κ, as it contains the process-specific matrix elements, while $\widehat{S}_N^\kappa$ depends on κ only via the color representations. The J_{κ_A} depend on whether κ_A is a quark or gluon that initiates the jet, and B_{κ_a,κ_b} each depend on the flavor of the initial-state partons κ_a and κ_b and the type of initial-state hadrons. The $\widehat{H}_N^\kappa$ and $\widehat{S}_N^\kappa$ are both matrices in the color space of κ which are traced over in eq. (5.7).

The precise form of the convolutions in eq. (5.7), as well as the definitions of the beam, jet, and soft functions, depends on the choice of jet and beam measures used in the N-jettiness observable. On the other hand, the hard function is not affected by these choices. So far, we have been using the observables $\widetilde{\mathcal{T}}_N^r$ without specifying the method of fixing the jet axes n_r. The form of the convolutions will generically depend on the jet axes choice. We discuss below the observables $\mathcal{T}_N^r$ obtained after the axes minimization in eq. (2.3). The factorization in eq. (5.7) holds for any jet axes choice that is within $\mathcal{O}(\lambda)$ of the minimized jet axes, where the power counting parameter λ is defined below.

5.2 Categorizing measures by power counting

To determine the structure of the convolutions in eq. (5.7), it is first instructive to form categories for the measures in table 1 that share common features in their convolution structure. In particular, we classify them by how they scale with the SCET power counting parameter $\lambda \ll 1$. Below, we use a light-cone decomposition of the momenta based on the jet axis n_A satisfying $n_A^2 = 0$ as well as the auxiliary vector $\bar{n}_A$ obeying $\bar{n}_A^2 = 0$ and $n_A \cdot \bar{n}_A = 2$.

An n_A-collinear mode within the A-th jet has momentum scaling as $(n_A \cdot p_i, \bar{n}_A \cdot p_i, p_i^{n_A\perp}) \sim \bar{n}_A \cdot p_i\,(\lambda^2, 1, \lambda)$. Here and below we use the label $\perp$ to refer to components perpendicular to the respective jet axis $\vec{n}_A$, while T indicates transverse momentum with respect to the beam. Considering all the jet measures in table 1, those with $\beta = 2$ have $\widetilde{\mathcal{T}}_N^{[n_A]} \sim \lambda^2$ (which includes the geometric measures), while those with $\beta = 1$ have $\widetilde{\mathcal{T}}_N^{[n_A]} \sim \lambda$. Since the components in the decomposition in eq. (5.5) scale homogeneously, the scaling of the corresponding soft momenta $\widetilde{\mathcal{T}}_N^{(A)[\mathrm{soft}]}$ must be the same as those of the corresponding collinear emissions. The soft momenta scale homogeneously, independent of the jet directions, so $p_s^\mu \sim \lambda^2$ for $\beta = 2$ and $p_s^\mu \sim \lambda$ for $\beta = 1$. The $\beta = 2$ situation is known as an $\mathrm{SCET_I}$ observable, while the $\beta = 1$ case is referred to as an $\mathrm{SCET_{II}}$ observable.

Since the convolutions in eq. (5.7) are always between observables with the same λ-scaling, we can classify the jet measures by whether they are in $\mathrm{SCET_I}$ or in $\mathrm{SCET_{II}}$. A similar classification can also be made for the beam measures. For collinear emissions along either of the two beams, $1/(2\cosh y_i) \simeq e^{-|y_i|}$ up to power corrections. All beam measures having this exponential rapidity dependence are in $\mathrm{SCET_I}$, while those measures with just

JHEP11(2015)072

p_{Ti} are in SCET$_{\rm II}$. Summarizing the scaling of the measures in table 1, we have:

SCET$_{\rm I}$ jets & beams:	Geometric(-R), Modified Geometric(-R), Conical Geometric ($\beta = \gamma = 2$);
SCET$_{\rm I}$ jets & SCET$_{\rm II}$ beams:	Conical ($\beta = 2$), XCone Default;
SCET$_{\rm II}$ jets & beams:	Conical ($\beta = 1$), Recoil-Free Default;
SCET$_{\rm II}$ jets & SCET$_{\rm I}$ beams:	Conical Geometric ($\beta = 1$, $\gamma = 2$),

(5.8)

though we have not made use of the last example in this paper.

Equation (5.5) for $\widetilde{\mathcal{T}}_N^r$ implies that the factorization theorem will have one convolution for each region it is differential in. For SCET$_{\rm I}$ cases we have convolutions in $(n_A \cdot p)$-momenta between the beam/jet functions and the soft function. In contrast, for SCET$_{\rm II}$ cases we have convolutions involving transverse or $\perp$-momenta between the beam/jet functions and the soft function. The homogeneous scaling for the components of N-jettiness also requires $\widetilde{\mathcal{T}}_N^{[n_r]} \sim \widetilde{\mathcal{T}}_N^{[n_{r'}]}$, such that all of the soft function convolution variables are of the same order in the power counting. If all jets and beams are in either SCET$_{\rm I}$ or SCET$_{\rm II}$, then that theory's ingredients can be used for the main components of the analysis. In the mixed case of SCET$_{\rm I}$ jets with SCET$_{\rm II}$ beams, the restriction on the radiation imposed by the measurement together with the power counting implies that the modes in the A-th jet can have parametrically larger $\perp$-momenta relative to their n_A axis than the modes in the beam do relative to the beam axis, since $p^i_{n_A\perp} \sim \lambda \gg p^i_{n_{a,b}\perp} \sim \lambda^2$.

One can also derive factorization theorems for N-jettiness measures with generic β. For any β such that $\beta - 1 \gg \lambda$ these measures fall in the SCET$_{\rm I}$ category, and they lead to β-dependent jet, beam, and soft functions. This is analogous to the factorization theorems derived in $e^+e^- \to$ dijets for general angularities [88, 89] and their recoil-free variants [27].[13] For simplicity we will not discuss the general β case here, but instead focus on the representative cases of $\beta = 1, 2$.

5.3 Impact of axes minimization

In general, the jet axes n_A need not align perfectly with the jet three-momenta $\vec{p}_A$, as long as the difference is $\mathcal{O}(\lambda)$. That said, the structure of the factorization theorem will simplify if we align the n_A axes within $\mathcal{O}(\lambda^2)$ of the jet direction. For jets defined with XCone, this alignment happens automatically for any of the $\beta = 2$ measures (including the XCone default), as explained near eq. (4.1) and discussed previously in ref. [7] (see also ref. [33, 50]). For this reason, we will focus the remainder of our discussion on jet measures in the SCET$_{\rm I}$ category, including the XCone default. This minimization implies that we are now discussing the specific N-jettiness observable $\mathcal{T}_N$ rather than the generic $\widetilde{\mathcal{T}}_N$.

The alignment of n_A with $\vec{p}_A$ means that the jet momentum has $\mathcal{O}(\lambda^2)$ perpendicular momentum relative to this axis. For all the geometric jet measures the perpendicular

[13] In the case of recoil-free angularities, there is a smooth interpolation between SCET$_{\rm I}$ and SCET$_{\rm II}$ as β goes from 2 to 1 [27].

JHEP11(2015)072

momentum is actually zero, and the component observables $\mathcal{T}_N^A$ then have a simple physical interpretation, since they measure the jet mass m_A^2 for each jet region via $\mathcal{T}_N^A = m_A^2/Q_A$ with $Q_A = 2\rho E_A$ [19]. For our XCone default measure the perpendicular momentum is $\mathcal{O}(\lambda^2)$, however this same physical interpretation still applies, with the only difference being that $Q_A = R^2 E_A/\cosh y_A$. On the other hand, for the conical geometric measure with $\beta = \gamma = 2$ there is not a precise relation between $\mathcal{T}_N^A$ and m_A^2, unless we were to adopt as an additional approximation $y_i \simeq y_A$.

Without aligning the jet axes and the jet three-momenta, the jet functions in the N-jettiness factorization theorem would depend on both $Q_A \widetilde{\mathcal{T}}_N^{[n_A]}$ and the total $p_{n_A\perp}$, such as in the jet function

$$J_{\kappa_A}\big(Q_A \widetilde{\mathcal{T}}_N^{[n_A]} - \vec{p}^{\,2}_{n_A\perp}, \mu\big). \tag{5.9}$$

Here, the two terms in J_{κ_A} are both $\mathcal{O}(\lambda^2)$, and κ_A indicates a quark or gluon. With the axes minimization, the dependence on the transverse momentum drops out, and this becomes simply

$$J_{\kappa_A}\big(Q_A \mathcal{T}_N^{[n_A]}, \mu\big). \tag{5.10}$$

These jet functions, which appear in the N-jettiness factorization theorem, are inclusive because the collinear radiation is always completely contained in the corresponding jet region. This means that they are a function of a single variable and do not depend on the jet boundary. However, the type of inclusive jet function we have does still depend on the jet measure. For instance, the geometric measures yield the standard inclusive hemisphere jet function, but we obtain a different inclusive jet function for the $\beta = \gamma = 2$ conical geometric measure.

5.4 Hadronic and partonic momentum conservation

The remaining ingredients that influence the form of the factorization theorem are momentum conservation and the choice of measurements X_N made on the jets and the nonhadronic particles. We will discuss the first issue here, before explaining why they impact the structure of the factorization theorem in the next subsection.

Momentum conservation says that

$$p^\mu_{\text{beam}} = p^\mu_a + p^\mu_b = q^\mu + \sum_A p^\mu_A\,, \tag{5.11}$$

where p_A^μ is the sum of all four-momenta for particles in region A, the $p^\mu_{a,b(\text{beam})}$ include the incoming proton momentum (momenta) minus the sum of the outgoing momentum of particles in the associated beam region, and q^μ is the total outgoing momentum of any nonhadronic particles. Even if the N-jettiness measurement specifies only a single beam region, we can divide the beam region in two by making an artificial split at zero rapidity into regions a and b. This split is useful for the discussion below, since it makes it simpler to talk about the two beam functions that are important for the dynamics of the beam region. We set $q^\mu = 0$ for cases where the final state does not involve nonhadronic particles.

JHEP11(2015)072

The largest $\mathcal{O}(\lambda^0)$ momentum component from each jet and beam region in eq. (5.11) can be extracted by projecting along the associated N-jettiness axis,

$$p_r^\mu = \omega_r \frac{n_r^\mu}{2} + \mathcal{O}(\lambda)\,. \tag{5.12}$$

This determines the variables appearing in the hard function

$$\widehat{H}_N = \widehat{H}_N(\{\omega_r n_r\}, q, \mu)\,, \tag{5.13}$$

where r runs over a, b, 1, …, N in the set of variables in $\{\cdots\}$.[14] These phase-space variables include things like the transverse momentum p_T^A and rapidity η_A of each jet, as well as the overall rapidity of all non-forward radiation Y which determines the boost of the partonic hard collision relative to the center-of-mass frame. These hard-function variables form the basis for the measurements we make on the jets as specified by $X_N(\Phi_N)$ in eq. (5.3) where $q_r = \omega_r n_r/2$. The variables are not all independent, since momentum conservation correlates the large $\mathcal{O}(\lambda^0)$ components of eq. (5.11). This is the same as imposing momentum conservation for the underlying hard partonic process with incoming and outgoing massless partons,

$$\omega_a \frac{n_a^\mu}{2} + \omega_b \frac{n_b^\mu}{2} = q^\mu + \sum_A \omega_A \frac{n_A^\mu}{2}\,. \tag{5.14}$$

In particular, this formula is used to compute $\widehat{H}_N$ when integrating out hard modes by matching QCD to SCET using calculations of S-matrix elements in the two theories. And this momentum conservation appears above in $\mathrm{d}\Phi_N$ in eq. (5.4). The same hard function in eq. (5.13) appears in the factorization theorem for exclusive jet cross sections for all choices of the N-jettiness jet and beam measures.

In eq. (5.14), the beam variables can be rewritten in terms of the total center-of-mass energy E_{cm} and momentum fractions $x_{a,b}$ for the colliding partons in the hard collision via $\omega_a = x_a E_{\mathrm{cm}}$ and $\omega_b = x_b E_{\mathrm{cm}}$. The jet variables ω_A are chosen so that $\omega_A = 2E_A + \mathcal{O}(\lambda)$, where E_A is the true jet energy, and the presence of $\mathcal{O}(\lambda)$ contributions in this relation ensure that eq. (5.14) is exactly satisfied. The presence of these $\mathcal{O}(\lambda)$ terms does not affect the evaluation of the hard function in eq. (5.13), where we may simply replace $\omega_A \to 2E_A$. This same replacement should be made in the formulas for the Q_A factors appearing in the jet functions, which are otherwise given by the results in table 3. However, the $\mathcal{O}(\lambda)$ terms can have implications for the convolutions between the jet, beam, and soft functions. To see explicitly how these $\mathcal{O}(\lambda)$ terms arise, it is convenient to project eq. (5.14) both along and transverse to the beam axis, giving

$$\omega_a = n_b \cdot q + \sum_A \omega_A \frac{n_b \cdot n_A}{2}\,, \qquad \omega_b = n_a \cdot q + \sum_A \omega_A \frac{n_a \cdot n_A}{2}\,, \tag{5.15}$$

$$0 = 2\,q_T^\mu + \sum_A \omega_A\, n_{AT}^\mu\,. \tag{5.16}$$

[14] To emphasize that $\widehat{H}_N$ can always be written in terms of Lorentz-invariant phase-space variables, one can rewrite this as $\widehat{H}_N(\{\omega_r\omega_{r'}\, n_r \cdot n_{r'}\}, \{\omega_r\, n_r \cdot q\}, q^2)$ with r and r' running over a, b, 1, …, N.

JHEP11(2015)072

	(Modified) Geometric	Geometric-R	Modified Geometric-R	XCone Default
$Q_A =$	$\rho_0\,\omega_A$	$\rho(R, y_A)\,\omega_A$	$\rho_C(R, y_A)\,\omega_A$	$\dfrac{R^2}{2\cosh y_A}\,\omega_A$

Table 3. Values of Q_A for various measures. The approximation $\omega_A = 2E_A$ is valid as long as the same replacement is made in the hard function.

The two equalities in eq. (5.15) simply fix $\omega_{a,b}$ regardless of how precisely we specify the jet axes n_A, the jet variables ω_A, or q^μ. This leaves the two constraints from eq. (5.16), which will be very important in the next subsection. These constraints involve n^μ_{AT}, which is determined by the azimuthal angle ϕ_{n_A} for the axis of each jet region, but they do not depend on the longitudinal (rapidity) component of n_A.

5.5 Convolutions from transverse momentum recoil

We now show how the two constraints in eq. (5.16) can influence the form of the convolutions appearing in the factorization theorem. Throughout this discussion, we assume that the jet axes n_A and jet three-momenta $\vec{p}_A$ are perfectly aligned, as is the case for the $\beta = 2$ measures with the minimized $\mathcal{T}_N$. We start with pure SCET_I observables before mentioning what happens with SCET_II beam measures.

To begin, imagine making highly granular measurements of the jet energies and directions with very fine p_T^A, η_A, and ϕ_A bins, as well as fully measuring the nonhadronic q^μ. In this situation, we have effectively completely measured the transverse vector q_T^μ, the jet energies E_A, and the vectors n_A, so we actually have a measurement that is sensitive to the $\mathcal{O}(\lambda)$ amount by which the ω_A variables differ from $2E_A$. Here, the A-th jet's momentum can be written as

$$p_A^\mu = (2E_A - n\cdot p_A)\frac{n_A^\mu}{2} + n\cdot p_A\,\frac{\bar{n}_A^\mu}{2} + p_{A\perp}^\mu\,, \tag{5.17}$$

where $n\cdot p_A \sim \mathcal{T}_N^A \sim \lambda^2$. We can therefore see that the components beyond $E_A n_A^\mu$ are $\mathcal{O}(\lambda^2)$ and do not have $\mathcal{O}(\lambda)$ projections on the axis transverse to the beam. If we consider transverse momentum conservation using the original momentum conservation in eq. (5.11), and insert eq. (5.17), then we find that the balance of transverse momenta at $\mathcal{O}(\lambda)$ is given by

$$k_T^\mu \equiv p_{aT}^\mu + p_{bT}^\mu = q_T^\mu + \sum_A E_A\, n_{AT}^\mu\,. \tag{5.18}$$

Using eq. (5.16) we can see that this is a small momentum $k_T^\mu \sim \lambda$. For the beam variables $p_{a,b}^\mu$, these $\mathcal{O}(\lambda)$ transverse components come from the transverse momenta of radiation emitted in the beam regions (since the transverse momenta in the proton are $\sim \Lambda_\text{QCD}$ which is much smaller). For the jet components, this $\mathcal{O}(\lambda)$ momentum comes from the mismatch between ω_A and $2E_A$, which we can see explicitly by using eq. (5.17) in eq. (5.16)

JHEP11(2015)072

to give

$$k_T^\mu = \sum_A \left(E_A - \frac{\omega_A}{2} \right) n_{AT}^\mu \,. \tag{5.19}$$

With the assumptions above, the constraint in eq. (5.18) is present because by making such a granular measurement, we have indirectly measured k_T^μ, and hence the total transverse momentum recoil of the beam radiation. This measurement therefore leads to p_T-dependent beam functions in the factorization theorem, which appear as

$$\int \mathrm{d}^2 p_T \, B_{\kappa_a}(t_a, x_a, \vec{p}_T, \mu) \, B_{\kappa_b}(t_b, x_b, \vec{k}_T - \vec{p}_T, \mu) \,. \tag{5.20}$$

Here $t_a = \omega_a \mathcal{T}_N^{[n_a]}$ and $t_b = \omega_b \mathcal{T}_N^{[n_b]}$ involve the variables that are convolved with the soft function. The double differential beam functions $B_{\kappa_a}(t_a, x_a, \vec{p}_T, \mu)$ were discussed in refs. [90, 91]. In ref. [21], examples where transverse momentum convolutions connect a jet and beam function were discussed for an $\mathrm{SCET_I}$ type 1-jettiness in deep inelastic scattering, and eq. (5.20) is the analog of the center-of-mass 1-jettiness variable considered there, except with the jet function replaced by a second beam function. The double differential factorization theorem with an explicit measurement of 0-jettiness and k_T in $\mathrm{SCET_I}$ was derived in ref. [92], and involves precisely the combination in eq. (5.20).

To obtain a simpler factorization theorem that does not involve p_T-dependent beam functions, we just have to perform a less granular measurement that does not constrain every aspect of the final state. For cases with external nonhadronic particles, the simplest approach is to not fully constrain all components of q_T^μ, for example by specifying q_T only within a bin centered on q_T^{central} with width $> \lambda q_T^{\text{central}}$. Since $\lambda \simeq m_A/E_A \simeq 0.1$, this corresponds to the typical size of bins that are already used in experimental analyses (unless they are only interested in measuring q_T). This method was used in ref. [15] when deriving the active-parton factorization theorem for beam thrust or 0-jettiness, where q_T was simply not measured. For beam thrust there are no jets, so $q_T^{\text{central}} = 0$, but this approach works equally well for $(N \geq 1)$-jettiness where $q_T^{\text{central}} \sim \lambda^0$ is large. Once one uses this coarser q_T binning, there are no other $\mathcal{O}(\lambda)$ constraints on the transverse momenta. In particular, specifying the bin for q_T yields an additional *unrestricted* integration over k_T^μ which appears in eq. (5.20) when deriving the factorization theorem. Therefore, we obtain independent transverse integrals over the two beam functions, $\int \mathrm{d}^2 p_T B_\kappa(t, x, \vec{p}_T, \mu) = B_\kappa(t, x, \mu)$, and only these p_T-independent beam functions appear in the N-jettiness factorization theorem, as in

$$B_{\kappa_a}(t_a, x_a, \mu) \, B_{\kappa_b}(t_b, x_b, \mu) \,. \tag{5.21}$$

Alternatively, for cases where $N \geq 2$, we can exploit the fact that we do not need to make finely-binned measurements of the jet energies or jet p_Ts. We can instead be satisfied with a measurement with center p_T^{central} in a bin of width $> \lambda p_T^{\text{central}}$, which could be for example using a bin centered at 500 GeV with width 50 GeV. This can be applied to both cases with $(q \neq 0)$ or without $(q = 0)$ additional nonhadronic particles. Since we can now

JHEP11(2015)072

vary by $\mathcal{O}(\lambda)$ at least two of the ω_A variables, we again loosen the constraint fixing k_T^μ and we can again freely integrate over this variable, and hence also obtain eq. (5.21). Both of these approaches to obtaining the simpler form of beam functions in eq. (5.21) require making less granular measurements when specifying X_N, but still remain fully sufficient for all standard LHC jet-style measurements. The only cases where eq. (5.20) become relevant is if we are actually interested in making a jet measurement so finely-binned that we can infer the small p_T spectrum of the beam radiation.

Just like for the jet function in eq. (5.10), the beam functions in eq. (5.21) are inclusive because collinear radiation along the beam directions is completely contained in the beam regions. Thus, they do not depend on the boundaries between the beam and jet regions. In principle, they could still depend on the beam measure, but because of eq. (3.11), for all the SCET_I beam measures we consider here, they are always given by the standard inclusive hemisphere beam functions [15, 93].

It is interesting to consider how the above arguments change if we maintain SCET_I measures for the jets (and aligned jet axes obtained from minimization) but now consider a SCET_II measure for the beam; this is the case encountered in the XCone default measure. In this situation, we still have inclusive jet functions that do not depend on $p_{n_A\perp}$ as in eq. (5.10). The key change is that now the N-jettiness measurement forces the beam transverse momenta to be smaller, $p_{aT}^\mu \sim p_{bT}^\mu \sim \lambda^2$, and the resulting SCET_II beam functions are of the broadening variety with $t_a = \mathcal{T}_N^{[n_a]}$ and $t_b = \mathcal{T}_N^{[n_b]}$ variables that are themselves $\mathcal{O}(\lambda^2)$. In addition to the renormalization scale μ, the beam functions depend on a rapidity renormalization scale ν, in the combination $\nu/\omega_{a,b}$. The ν scale is needed to sum logarithms associated with rapidity divergences that appear from the separation of modes in the beam and soft functions [94, 95]. From eq. (5.18), we must also have $k_T^\mu = p_{aT}^\mu + p_{bT}^\mu = q_T^\mu + \sum_A E_A n_{AT}^\mu \sim \lambda^2$. Once again we can integrate over k_T^μ either by considering a bin for q_T^μ or a bin for two of the jet energies E_A. In this case, the bins need only have a size of $> \lambda^2 q_T^{\text{central}}$ or $> \lambda^2 E_A^{\text{central}}$ in order to sufficiently integrate over k_T^μ such that we get p_T-independent beam functions, as in eq. (5.21).

5.6 Factorization theorems for N-jettiness

We now have all the ingredients needed to assemble the factorization theorem for N-jettiness for various jet and beam measures. For jet and beam measures in SCET_I, the mathematical derivation of this factorization theorem follows closely the detailed derivation given for beam thrust in ref. [15], or for DIS 1-jettiness in ref. [21], which we therefore will not bother to repeat here. The N-jet case has also been discussed in some detail in refs. [16, 30]. The required ingredients in the derivation have all been discussed in the previous subsections.

With jet and beam measures in the SCET_I category, axes determined by minimization, and the choice for X_N that does not directly or indirectly measure the transverse

JHEP11(2015)072

momentum of the beam radiation, the factorization theorem in eq. (5.7) becomes

$$\begin{aligned}
&\frac{\mathrm{d}\sigma_\kappa(\Phi_N)}{\mathrm{d}\mathcal{T}_N^a \mathrm{d}\mathcal{T}_N^b \mathrm{d}\mathcal{T}_N^1 \cdots \mathrm{d}\mathcal{T}_N^N} \\
&\quad = \mathrm{tr}\, \widehat{H}_N^\kappa(\{\omega_r n_r\}, q, \mu) \int \biggl[\prod_r \mathrm{d}\mathcal{T}_N^{[n_r]}\biggr] \omega_a B_{\kappa_a}\bigl(\omega_a \mathcal{T}_N^{[n_a]}, x_a, \mu\bigr)\, \omega_b B_{\kappa_b}\bigl(\omega_b \mathcal{T}_N^{[n_b]}, x_b, \mu\bigr) \\
&\qquad \times Q_1 J_{\kappa_1}\bigl(Q_1 \mathcal{T}_N^{[n_1]}, \mu\bigr) \cdots Q_N J_{\kappa_N}\bigl(Q_N\, \mathcal{T}_N^{[n_N]}, \mu\bigr)\, \widehat{S}_N^\kappa\biggl(\{\mathcal{T}_N^r - \mathcal{T}_N^{[n_r]}\}, \biggl\{\frac{\omega_r n_r}{Q_r}\biggr\}, \mu\biggr)\,,
\end{aligned} \tag{5.22}$$

where r and $r' = a, b, 1, \ldots, N$ and all of the convolutions are now made explicit. Here, the soft function $\widehat{S}_N^\kappa$ depends on the $N+2$ observables $\mathcal{T}_N^r$. It is a scalar function of the variables $\{\omega_r n_r^\mu / Q_r\}$, which encode the dependence on the angles between various beam and jet directions through their dot products. Although not indicated by our notation, the soft function also depends on the size and shape of the jet regions through the precise definition of the jet and beam measures used to define these observables. Both the jet functions and beam functions in eq. (5.22) are of the inclusive variety, and hence do not depend on the boundaries between the jet or beam regions. The beam functions also contain the nonperturbative parton distributions $f_j(\xi, \mu)$ through a factorization from the perturbative radiation into calculable coefficients $\mathcal{I}_{ij}$ [15, 93, 96],

$$B_i(\omega k, x, \mu) = \sum_j \int_x^1 \frac{\mathrm{d}z}{z}\, \mathcal{I}_{ij}(\omega k, z, \mu)\, f_j\biggl(\frac{x}{z}, \mu\biggr)\,. \tag{5.23}$$

With geometric (and related) measures, eq. (5.22) was the version of the 1-jettiness factorization theorem used for the analysis in ref. [19].

For the various geometric measures, the Q_A factors needed for eq. (5.22) are given above in table 3. For the $\beta = \gamma = 2$ conical geometric measure we let $Q_A = R^2 \omega_A$. For this measure, the inclusive jet functions become $J_{\kappa_A}(Q_A \mathcal{T}_N^{[n_A]}, y_A, \mu)$ in eq. (5.25), due to the $\cosh y_A / \cosh y_i$ weighting factor in the jet measure. Thus, they are not just the standard hemisphere jet functions. Similarly, for this case we also will have a soft function that can depend on the y_A variables.

In eq. (5.22) we are differential in two beam regions, $\mathcal{T}_N^a$ and $\mathcal{T}_N^b$. If we only want to consider a single beam region and measurement observable $\mathcal{T}_N^{\mathrm{beam}} = \mathcal{T}_N^a + \mathcal{T}_N^b$, then it is possible to simplify the form of the factorization theorem. Using the corresponding collinear projection, $\mathcal{T}_N^{a[n_a]} + \mathcal{T}_N^{b[n_b]} = \mathcal{T}_N^{[n_{\mathrm{beam}}]}$, yields a "double-beam function" for $\mathrm{SCET_I}$ measures

$$\begin{aligned}
&BB_{ij}(\omega_a \mathcal{T}_N^{[n_{\mathrm{beam}}]}, \omega_b \mathcal{T}_N^{[n_{\mathrm{beam}}]}, x_a, x_b, \mu) \\
&\qquad = \omega_a \omega_b \int \mathrm{d}k\, B_i\bigl(\omega_a k, x_a, \mu\bigr)\, B_j\bigl(\omega_b(\mathcal{T}_N^{[n_{\mathrm{beam}}]} - k), x_b, \mu\bigr)\,.
\end{aligned} \tag{5.24}$$

Projecting the soft function in the same way, using $\mathcal{T}_N^{a[\mathrm{soft}]} + \mathcal{T}_N^{b[\mathrm{soft}]} = \mathcal{T}_N^{\mathrm{beam}[\mathrm{soft}]}$, this

JHEP11(2015)072

reduces eq. (5.22) to

$$\begin{aligned}\frac{\mathrm{d}\sigma_\kappa(\Phi_N)}{\mathrm{d}\mathcal{T}_N^{\mathrm{beam}}\mathrm{d}\mathcal{T}_N^1\cdots\mathrm{d}\mathcal{T}_N^N} &= \mathrm{tr}\,\widehat{H}_N^\kappa(\{\omega_r n_r\},q,\mu)\int\biggl[\prod_r d\mathcal{T}_N^{[n_r]}\biggr]BB_{\kappa_a\kappa_b}\bigl(\omega_a\mathcal{T}_N^{[n_{\mathrm{beam}}]},\omega_b\mathcal{T}_N^{[n_{\mathrm{beam}}]},x_a,x_b,\mu\bigr)\\ &\quad\times Q_1 J_{\kappa_1}\bigl(Q_1\,\mathcal{T}_N^{[n_1]},\mu\bigr)\cdots Q_N J_{\kappa_N}\bigl(Q_N\,\mathcal{T}_N^{[n_N]},\mu\bigr)\,\widehat{S}_N^{\kappa(\mathrm{I})}\biggl(\{\mathcal{T}_N^r-\mathcal{T}_N^{[n_r]}\},\biggl\{\frac{\omega_r n_r}{Q_r}\biggr\},\mu\biggr),\end{aligned} \tag{5.25}$$

where now $r=\mathrm{beam},1,\ldots,N$. For the modified geometric(-R) measure, the soft function $\widehat{S}_N^{\kappa(\mathrm{I})}$ in eq. (5.25) has a C-parameter-type measurement for its $\mathcal{T}_N^{\mathrm{beam}}$ observable and thrust-type measurements for the jet observables $\mathcal{T}_N^A$, and eq. (5.25) involves the standard inclusive hemisphere jet functions.

Next, we consider the mixed measure case, with $\mathrm{SCET_I}$ jet measures and $\mathrm{SCET_{II}}$ beam measures, still with jet axes determined by minimization and a choice of X_N that is insensitive to transverse momentum of the beam radiation. For this case, there has not yet been any literature providing a detailed mathematical derivation of a factorization theorem. Factorization theorems have been worked out for pure $\mathrm{SCET_{II}}$ measurements of event shapes in $e^+e^-\to$ dijets [27, 94, 95, 97, 98], and active-parton factorization theorems have also been derived for $pp\to H$ with an E_T jet veto [99] or p_T^{jet} veto [99–103]; see also [104] for transverse thrust. Experience from these results enables us to anticipate the form of the convolutions that will appear between the beam and soft functions in the mixed measure N-jettiness case. So even though the complete derivation of the factorization theorem for this case is beyond the scope of this work, we can still put the information collected above together to anticipate its structure.

For $\mathrm{SCET_{II}}$ beam measures we expect the double-beam function to be given by

$$BB_{ij}\biggl(k,x_a,x_b,\mu,\frac{\nu}{\omega_a},\frac{\nu}{\omega_b}\biggr)=\int\mathrm{d}k'\,B_i\biggl(k',x_a,\mu,\frac{\nu}{\omega_a}\biggr)\,B_j\biggl(k-k',x_b,\mu,\frac{\nu}{\omega_b}\biggr). \tag{5.26}$$

The individual beam functions here are of the broadening type and involve the rapidity scale parameter ν [95]. For $\mathrm{SCET_I}$ jet measures and a single $\mathrm{SCET_{II}}$ beam measure we then expect a factorization theorem of the form

$$\begin{aligned}\frac{\mathrm{d}\sigma_\kappa(\Phi_N)}{\mathrm{d}\mathcal{T}_N^{\mathrm{beam}}\mathrm{d}\mathcal{T}_N^1\cdots\mathrm{d}\mathcal{T}_N^N} &= \mathrm{tr}\,\widehat{H}_N^\kappa(\{\omega_r n_r\},q,\mu)\int\biggl[\prod_r \mathrm{d}\mathcal{T}_N^{[n_r]}\biggr]BB_{\kappa_a\kappa_b}\biggl(\mathcal{T}_N^{[n_{\mathrm{beam}}]},x_a,x_b,\mu,\frac{\nu}{\omega_a},\frac{\nu}{\omega_b}\biggr)\\ &\quad\times Q_1 J_{\kappa_1}\bigl(Q_1\,\mathcal{T}_N^{[n_1]},\mu\bigr)\cdots Q_N J_{\kappa_N}\bigl(Q_N\,\mathcal{T}_N^{[n_N]},\mu\bigr)\,\widehat{S}_N^{\kappa(\mathrm{I/II})}\\ &\quad\times\biggl(\{\mathcal{T}_N^r-\mathcal{T}_N^{[n_r]}\},\biggl\{\frac{\omega_r n_r}{Q_r}\biggr\},\mu,\frac{\nu}{\mu}\biggr).\end{aligned} \tag{5.27}$$

This is the factorization formula that is relevant for the XCone default measure, with the Q_A factors given above in table 3. Note that here the soft function $\widehat{S}_N^{\kappa(\mathrm{I/II})}$ has broadening-type variables convolved with the beam functions, and has dependence on the scale ν

JHEP11(2015)072

which compensates the ν dependence in the double-beam function. The conical measure with $\beta = 2$ will have an analogous factorization theorem but requires different jet and soft functions that take into account that the jet measure cannot be written as $n \cdot p_i \, \omega_A / Q_A$ with some Q_A. We leave a detailed mathematical analysis and proof of the active-parton factorization theorem in eq. (5.27) to future work. It will also be interesting to test it against fixed-order predictions for these N-jettiness distributions.

The other main class of measures in table 1 are those that have both jet and beam measures in the SCET_{II} category. This includes the recoil-free default XCone measure, as well as the conical measure with $\beta = 1$. Once again there has not yet been a detailed mathematical analysis of this case in the literature, but from our previous analysis and from experience with simpler cases, we can anticipate the form of the associated factorization theorem. With axes determined by minimization, and with a choice of X_N that is again insensitive to the total transverse momentum of the beam radiation, we expect the appropriate factorization theorem to contain the same SCET_{II} double-beam function in eq. (5.26) with no additional recoil convolutions. This would be analogous to the factorization theorem for recoil-free broadening in e^+e^- collisions in ref. [27]. In contrast to eq. (5.27), the jet functions must now be of the broadening type and likely also depend on a rapidity scale ν. The corresponding soft function $S_N^{\kappa(\text{II})}$ now only depends on convolution variables of the broadening type and has to cancel the ν dependence of both beam and jet functions. We again leave a detailed mathematical analysis and proof of the active-parton factorization theorem for this case to future work.

6 Conclusions

In this paper, we introduced the new XCone jet algorithm, which is based on the N-jettiness event shape. XCone is an exclusive cone algorithm that finds a fixed predefined number of jets. Exploiting the measure flexibility inherent to N-jettiness, we defined a new conical geometric measure that combines the geometric measure, which is theoretically motivated and preferred, with the conical measure, which has already been proven to be experimentally robust in the context of jet substructure techniques using N-subjettiness. In a companion paper [1], we present three physics case studies to highlight how XCone can be beneficial to a variety of LHC analyses. In particular, XCone is capable of resolving overlapping jets without requiring a separate split/merge step, and allows for a continuous transition from the resolved regime of well separated jets to the boosted regime of overlapping jets.

Our focus in this paper was on the case $\gamma = 1$, for which the beam measure scales as p_T, such that $\mathcal{T}_N$ minimization is roughly the same as minimizing the total unclustered p_T. By changing γ, one changes whether jets are found preferentially in the central or forward parts of the detector. In the future, it would be interesting to study the impact and utility of different γ values, especially $\gamma = 2$ which is the natural value from the original geometric measure. At present, the XCone code is limited to $\gamma = 1$, primarily because our method to find seed axes employs the existing longitudinally-invariant generalized k_T algorithm. It is possible to build recursive clustering algorithms optimized to find seed axes for any given $\mathcal{T}_N$ measure, which is planned for future work.

JHEP11(2015)072

In constructing the XCone algorithm, we have chosen a specific measure for both the N-jettiness partitioning into jet and beam regions as well as the jet axis finding via the overall N-jettiness minimization. This has lead to an interesting compromise, where in order for the XCone default measure to use dot-product distances in the jet partitioning, the jet regions could not be perfectly stable cones (meaning the jet axis is not exactly aligned with the total jet momentum). One could imagine loosening the requirement of $\mathcal{T}_N$ minimization, though, to define an array of exclusive jet algorithms. Following the idea that jet axis finding and jet region finding can be regarded as two distinct steps, one could use any exclusive clustering algorithm to find jet axes and only use $\mathcal{T}_N$ for defining the jet partitions. Alternatively, if one wants the jet axis to be perfectly aligned with the jet momentum, one could build an exclusive cone jet algorithm that directly searches for N mutually stable perfect cones. More generally, it is worth reexamining the potential of exclusive jet algorithms at hadron colliders, and XCone provides a clear proof of concept with interesting physics applications [1].

Beyond just being an exclusive jet algorithm that finds a fixed number of jets, XCone can be adapted to become an inclusive jet algorithm that finds a variable number of jets by analyzing the distribution of $\mathcal{T}_N$ for different N. For an event with M jets, $\mathcal{T}_N$ should be large when $N < M$ and small when $N \geq M$, producing a sharp downward transition in the value of $\mathcal{T}_N$ when $N = M$. Therefore, one could iteratively increase the value of N until $\mathcal{T}_N$ undergoes this transition, either by measuring the "slope" $\mathrm{d}\mathcal{T}_N/\mathrm{d}N$ or by imposing a fixed $\mathcal{T}_{\mathrm{cut}}$.[15] Using XCone as an inclusive jet algorithm could potentially be useful for jet counting in event samples with a variable number of jets, for accurate event reconstruction in the face of hard initial state radiation, or for improving background discrimination by dividing an event sample into exclusive N-jet bins.

Finally, we anticipate that the XCone default measure will be used in future N-jettiness theoretical calculations. Since XCone is IRC safe, there are no obstacles for performing fixed-order or resummed calculations for any of the measures studied here. While jet and beam measures that are linear in the particle momenta (like the XCone default measure) are simplest when using factorization to carry out calculations, the discussion in section 5 implies that the same SCET-based methods can also be applied for other measures. Ultimately, we look forward to comparing precision XCone-based calculations to precision XCone-based measurements at the LHC.

Acknowledgments

We thank Daniele Bertolini, Matteo Cacciari, Steve Ellis, Duff Neill, Gavin Salam, Gregory Soyez, Wouter Waalewijn, and Ken Van Tilburg for helpful conversations. This work was supported by the Offices of Nuclear and Particle Physics of the U.S. Department of Energy (DOE) under Contracts DE-SC00012567 and DE-SC0011090. I.S. is also supported by the Simons Foundation Investigator grant 327942. F.T. is also supported by the DFG Emmy-Noether Grant No. TA 867/1-1. J.T. is also supported by the DOE Early Career research program DE-SC0006389 and by a Sloan Research Fellowship from the Alfred P.

[15] Because XCone only finds a local minimum by default, there is no guarantee that $\mathcal{T}_N$ is a strictly decreasing function of N, though in practice this is a small effect when using the heuristic in eq. (4.10).

JHEP11(2015)072

Sloan Foundation. C.V. is also supported by the U.S. National Science Foundation under Grant Nos. NSF-PHY-0705682, NSF-PHY-0969510 (LHC Theory Initiative). T.W. is also supported by the MIT Undergraduate Research Opportunities Program (UROP) through the Paul E. Gray Endowed Fund.

References

[1] J. Thaler and T.F. Wilkason, *Resolving boosted jets with XCone*, arXiv:1508.01518 [INSPIRE].

[2] S.D. Ellis, J. Huston, K. Hatakeyama, P. Loch and M. Tonnesmann, *Jets in hadron-hadron collisions*, *Prog. Part. Nucl. Phys.* **60** (2008) 484 [arXiv:0712.2447] [INSPIRE].

[3] G.P. Salam, *Towards jetography*, *Eur. Phys. J.* **C 67** (2010) 637 [arXiv:0906.1833] [INSPIRE].

[4] M. Cacciari, G.P. Salam and G. Soyez, *The anti-k_t jet clustering algorithm*, *JHEP* **04** (2008) 063 [arXiv:0802.1189] [INSPIRE].

[5] I.W. Stewart, F.J. Tackmann and W.J. Waalewijn, *N-jettiness: an inclusive event shape to veto jets*, *Phys. Rev. Lett.* **105** (2010) 092002 [arXiv:1004.2489] [INSPIRE].

[6] J. Thaler and K. Van Tilburg, *Identifying boosted objects with N-subjettiness*, *JHEP* **03** (2011) 015 [arXiv:1011.2268] [INSPIRE].

[7] J. Thaler and K. Van Tilburg, *Maximizing boosted top identification by minimizing N-subjettiness*, *JHEP* **02** (2012) 093 [arXiv:1108.2701] [INSPIRE].

[8] S. Catani, Y.L. Dokshitzer, M.H. Seymour and B.R. Webber, *Longitudinally invariant k_t clustering algorithms for hadron hadron collisions*, *Nucl. Phys.* **B 406** (1993) 187 [INSPIRE].

[9] M. Cacciari and G.P. Salam, *Pileup subtraction using jet areas*, *Phys. Lett.* **B 659** (2008) 119 [arXiv:0707.1378] [INSPIRE].

[10] M. Cacciari, G.P. Salam and G. Soyez, *The catchment area of jets*, *JHEP* **04** (2008) 005 [arXiv:0802.1188] [INSPIRE].

[11] A. Abdesselam et al., *Boosted objects: a probe of beyond the standard model physics*, *Eur. Phys. J.* **C 71** (2011) 1661 [arXiv:1012.5412] [INSPIRE].

[12] A. Altheimer et al., *Jet substructure at the Tevatron and LHC: new results, new tools, new benchmarks*, *J. Phys.* **G 39** (2012) 063001 [arXiv:1201.0008] [INSPIRE].

[13] A. Altheimer et al., *Boosted objects and jet substructure at the LHC. Report of BOOST2012, held at IFIC Valencia, 23rd-27th of July 2012*, *Eur. Phys. J.* **C 74** (2014) 2792 [arXiv:1311.2708] [INSPIRE].

[14] D. Adams et al., *Towards an understanding of the correlations in jet substructure*, *Eur. Phys. J.* **C 75** (2015) 409 [arXiv:1504.00679] [INSPIRE].

[15] I.W. Stewart, F.J. Tackmann and W.J. Waalewijn, *Factorization at the LHC: from PDFs to initial state jets*, *Phys. Rev.* **D 81** (2010) 094035 [arXiv:0910.0467] [INSPIRE].

JHEP11(2015)072

[16] T.T. Jouttenus, I.W. Stewart, F.J. Tackmann and W.J. Waalewijn, *The soft function for exclusive N-jet production at hadron colliders*, *Phys. Rev.* **D 83** (2011) 114030 [arXiv:1102.4344] [INSPIRE].

[17] J.-H. Kim, *Rest frame subjet algorithm with SISCone jet for fully hadronic decaying Higgs search*, *Phys. Rev.* **D 83** (2011) 011502 [arXiv:1011.1493] [INSPIRE].

[18] C.W. Bauer, F.J. Tackmann, J.R. Walsh and S. Zuberi, *Factorization and resummation for dijet invariant mass spectra*, *Phys. Rev.* **D 85** (2012) 074006 [arXiv:1106.6047] [INSPIRE].

[19] T.T. Jouttenus, I.W. Stewart, F.J. Tackmann and W.J. Waalewijn, *Jet mass spectra in Higgs boson plus one jet at next-to-next-to-leading logarithmic order*, *Phys. Rev.* **D 88** (2013) 054031 [arXiv:1302.0846] [INSPIRE].

[20] I.W. Stewart, F.J. Tackmann and W.J. Waalewijn, *Dissecting soft radiation with factorization*, *Phys. Rev. Lett.* **114** (2015) 092001 [arXiv:1405.6722] [INSPIRE].

[21] D. Kang, C. Lee and I.W. Stewart, *Using 1-jettiness to measure 2 jets in DIS 3 ways*, *Phys. Rev.* **D 88** (2013) 054004 [arXiv:1303.6952] [INSPIRE].

[22] Z.-B. Kang, X. Liu and S. Mantry, *1-jettiness DIS event shape: NNLL+NLO results*, *Phys. Rev.* **D 90** (2014) 014041 [arXiv:1312.0301] [INSPIRE].

[23] Z.-B. Kang, S. Mantry and J.-W. Qiu, *N-jettiness as a probe of nuclear dynamics*, *Phys. Rev.* **D 86** (2012) 114011 [arXiv:1204.5469] [INSPIRE].

[24] Z.-B. Kang, X. Liu, S. Mantry and J.-W. Qiu, *Probing nuclear dynamics in jet production with a global event shape*, *Phys. Rev.* **D 88** (2013) 074020 [arXiv:1303.3063] [INSPIRE].

[25] D. Kang, C. Lee and I.W. Stewart, *Analytic calculation of 1-jettiness in DIS at $\mathcal{O}(\alpha_s)$*, *JHEP* **11** (2014) 132 [arXiv:1407.6706] [INSPIRE].

[26] Z.-B. Kang, X. Liu, S. Mantry and J. Qiu, *The 1-jettiness DIS spectrum: factorization, resummation and jet algorithm dependence*, arXiv:1503.04210 [INSPIRE].

[27] A.J. Larkoski, D. Neill and J. Thaler, *Jet shapes with the broadening axis*, *JHEP* **04** (2014) 017 [arXiv:1401.2158] [INSPIRE].

[28] S. Alioli et al., *Combining higher-order resummation with multiple NLO calculations and parton showers in GENEVA*, *JHEP* **09** (2013) 120 [arXiv:1211.7049] [INSPIRE].

[29] R. Boughezal, C. Focke, X. Liu and F. Petriello, *W-boson production in association with a jet at next-to-next-to-leading order in perturbative QCD*, *Phys. Rev. Lett.* **115** (2015) 062002 [arXiv:1504.02131] [INSPIRE].

[30] J. Gaunt, M. Stahlhofen, F.J. Tackmann and J.R. Walsh, *N-jettiness subtractions for NNLO QCD calculations*, *JHEP* **09** (2015) 058 [arXiv:1505.04794] [INSPIRE].

[31] G.F. Sterman and S. Weinberg, *Jets from quantum chromodynamics*, *Phys. Rev. Lett.* **39** (1977) 1436 [INSPIRE].

[32] G.C. Blazey et al., *Run II jet physics*, hep-ex/0005012 [INSPIRE].

[33] S.D. Ellis, J. Huston and M. Tonnesmann, *On building better cone jet algorithms*, *eConf* **C 010630** (2001) 513 [hep-ph/0111434] [INSPIRE].

[34] G.P. Salam and G. Soyez, *A practical seedless infrared-safe cone jet algorithm*, *JHEP* **05** (2007) 086 [arXiv:0704.0292] [INSPIRE].

[35] C.F. Berger et al., *Snowmass 2001: jet energy flow project*, *eConf* **C 010630** (2001) P512 [hep-ph/0202207] [INSPIRE].

JHEP11(2015)072

[36] L. Angelini et al., *Jet analysis by deterministic annealing*, *Phys. Lett.* **B 545** (2002) 315 [hep-ph/0207032] [INSPIRE].

[37] L. Angelini, G. Nardulli, L. Nitti, M. Pellicoro, D. Perrino and S. Stramaglia, *Deterministic annealing as a jet clustering algorithm in hadronic collisions*, *Phys. Lett.* **B 601** (2004) 56 [hep-ph/0407214] [INSPIRE].

[38] D. Yu. Grigoriev, E. Jankowski and F.V. Tkachov, *Towards a standard jet definition*, *Phys. Rev. Lett.* **91** (2003) 061801 [hep-ph/0301185] [INSPIRE].

[39] D. Yu. Grigoriev, E. Jankowski and F.V. Tkachov, *Optimal jet finder*, *Comput. Phys. Commun.* **155** (2003) 42 [hep-ph/0301226] [INSPIRE].

[40] S. Chekanov, *A new jet algorithm based on the k-means clustering for the reconstruction of heavy states from jets*, *Eur. Phys. J.* **C 47** (2006) 611 [hep-ph/0512027] [INSPIRE].

[41] Y.-S. Lai and B.A. Cole, *Jet reconstruction in hadronic collisions by gaussian filtering*, arXiv:0806.1499 [INSPIRE].

[42] I. Volobouev, *FFTJet: a package for multiresolution particle jet reconstruction in the Fourier domain*, arXiv:0907.0270 [INSPIRE].

[43] L. Mackey, B. Nachman, A. Schwartzman and C. Stansbury, *Fuzzy jets*, arXiv:1509.02216 [INSPIRE].

[44] G.F. Sterman, *Summation of large corrections to short distance hadronic cross-sections*, *Nucl. Phys.* **B 281** (1987) 310 [INSPIRE].

[45] S. Catani and L. Trentadue, *Resummation of the QCD perturbative series for hard processes*, *Nucl. Phys.* **B 327** (1989) 323 [INSPIRE].

[46] G.P. Korchemsky and G.F. Sterman, *Infrared factorization in inclusive B meson decays*, *Phys. Lett.* **B 340** (1994) 96 [hep-ph/9407344] [INSPIRE].

[47] H. Georgi, *A simple alternative to jet-clustering algorithms*, arXiv:1408.1161 [INSPIRE].

[48] S.-F. Ge, *The Georgi algorithms of jet clustering*, *JHEP* **05** (2015) 066 [arXiv:1408.3823] [INSPIRE].

[49] Y. Bai, Z. Han and R. Lu, *J_{E_T}: a global jet finding algorithm*, *JHEP* **03** (2015) 102 [arXiv:1411.3705] [INSPIRE].

[50] J. Thaler, *Jet maximization, axis minimization and stable cone finding*, *Phys. Rev.* **D 92** (2015) 074001 [arXiv:1506.07876] [INSPIRE].

[51] E. Farhi, *A QCD test for jets*, *Phys. Rev. Lett.* **39** (1977) 1587 [INSPIRE].

[52] H. Georgi and M. Machacek, *A simple QCD prediction of jet structure in e^+e^- annihilation*, *Phys. Rev. Lett.* **39** (1977) 1237 [INSPIRE].

[53] S. Brandt and H. Dahmen, *Axes and scalar measures of two-jet and three-jet events*, *Z. Phys.* **C 1** (1979) 61.

[54] S.P. Lloyd, *Least squares quantization in PCM*, *IEEE Trans. Inf. Theor.* **28** (1982) 129.

[55] C. Ding, D. Zhou, X. He and H. Zha, *R1-pca: rotational invariant ℓ^1-norm principal component analysis for robust subspace factorization*, in proceedings of the 23rd *international conference on Machine learning (ICML06)*, June 25–29, New York, U.S.A. (2006).

JHEP11(2015)072

[56] S.D. Ellis and D.E. Soper, *Successive combination jet algorithm for hadron collisions*, *Phys. Rev.* **D 48** (1993) 3160 [hep-ph/9305266] [INSPIRE].

[57] Y.L. Dokshitzer, G.D. Leder, S. Moretti and B.R. Webber, *Better jet clustering algorithms*, *JHEP* **08** (1997) 001 [hep-ph/9707323] [INSPIRE].

[58] M. Wobisch and T. Wengler, *Hadronization corrections to jet cross-sections in deep inelastic scattering*, hep-ph/9907280 [INSPIRE].

[59] M. Wobisch, *Measurement and QCD analysis of jet cross-sections in deep inelastic positron proton collisions at* $\sqrt{s} = 300$ *GeV*, DESY-THESIS-2000-049 (2000).

[60] A.J. Larkoski and J. Thaler, *Aspects of jets at* 100 *TeV*, *Phys. Rev.* **D 90** (2014) 034010 [arXiv:1406.7011] [INSPIRE].

[61] D. Bertolini, T. Chan and J. Thaler, *Jet observables without jet algorithms*, *JHEP* **04** (2014) 013 [arXiv:1310.7584] [INSPIRE].

[62] G. Salam, E_i^∞ *scheme*, unpublished.

[63] M. Cacciari, G.P. Salam and G. Soyez, *FastJet user manual*, *Eur. Phys. J.* **C 72** (2012) 1896 [arXiv:1111.6097] [INSPIRE].

[64] *Fastjet contrib*, http://fastjet.hepforge.org/contrib/.

[65] G. Soyez, G.P. Salam, J. Kim, S. Dutta and M. Cacciari, *Pileup subtraction for jet shapes*, *Phys. Rev. Lett.* **110** (2013) 162001 [arXiv:1211.2811] [INSPIRE].

[66] R. Boughezal, X. Liu and F. Petriello, *N-jettiness soft function at next-to-next-to-leading order*, *Phys. Rev.* **D 91** (2015) 094035 [arXiv:1504.02540] [INSPIRE].

[67] G. Parisi, *Super inclusive cross-sections*, *Phys. Lett.* **B 74** (1978) 65 [INSPIRE].

[68] J.F. Donoghue, F.E. Low and S.-Y. Pi, *Tensor analysis of hadronic jets in quantum chromodynamics*, *Phys. Rev.* **D 20** (1979) 2759 [INSPIRE].

[69] S. Catani and B.R. Webber, *Resummed C parameter distribution in* e^+e^- *annihilation*, *Phys. Lett.* **B 427** (1998) 377 [hep-ph/9801350] [INSPIRE].

[70] E. Gardi and L. Magnea, *The C parameter distribution in* e^+e^- *annihilation*, *JHEP* **08** (2003) 030 [hep-ph/0306094] [INSPIRE].

[71] G.P. Korchemsky and S. Tafat, *On power corrections to the event shape distributions in QCD*, *JHEP* **10** (2000) 010 [hep-ph/0007005] [INSPIRE].

[72] A.H. Hoang, D.W. Kolodrubetz, V. Mateu and I.W. Stewart, *C-parameter distribution at* N^3LL' *including power corrections*, *Phys. Rev.* **D 91** (2015) 094017 [arXiv:1411.6633] [INSPIRE].

[73] S. Gangal, M. Stahlhofen and F.J. Tackmann, *Rapidity-dependent jet vetoes*, *Phys. Rev.* **D 91** (2015) 054023 [arXiv:1412.4792] [INSPIRE].

[74] S. Catani, G. Turnock and B.R. Webber, *Jet broadening measures in* e^+e^- *annihilation*, *Phys. Lett.* **B 295** (1992) 269 [INSPIRE].

[75] Y.L. Dokshitzer, A. Lucenti, G. Marchesini and G.P. Salam, *On the QCD analysis of jet broadening*, *JHEP* **01** (1998) 011 [hep-ph/9801324] [INSPIRE].

[76] A. Banfi, G.P. Salam and G. Zanderighi, *Principles of general final-state resummation and automated implementation*, *JHEP* **03** (2005) 073 [hep-ph/0407286] [INSPIRE].

JHEP11(2015)072

[77] A.J. Larkoski, G.P. Salam and J. Thaler, *Energy correlation functions for jet substructure*, *JHEP* **06** (2013) 108 [arXiv:1305.0007] [INSPIRE].

[78] J.M. Butterworth, J.P. Couchman, B.E. Cox and B.M. Waugh, *KtJet: a C++ implementation of the K-perpendicular clustering algorithm*, *Comput. Phys. Commun.* **153** (2003) 85 [hep-ph/0210022] [INSPIRE].

[79] M. Boronat, J. Fuster, I. Garcia, E. Ros and M. Vos, *A robust jet reconstruction algorithm for high-energy lepton colliders*, *Phys. Lett.* **B 750** (2015) 95 [arXiv:1404.4294] [INSPIRE].

[80] J.C. Collins, D.E. Soper and G.F. Sterman, *Soft gluons and factorization*, *Nucl. Phys.* **B 308** (1988) 833 [INSPIRE].

[81] J.R. Gaunt, *Glauber gluons and multiple parton interactions*, *JHEP* **07** (2014) 110 [arXiv:1405.2080] [INSPIRE].

[82] M. Zeng, *Drell-Yan process with jet vetoes: breaking of generalized factorization*, *JHEP* **10** (2015) 189 [arXiv:1507.01652] [INSPIRE].

[83] C.W. Bauer, S. Fleming and M.E. Luke, *Summing Sudakov logarithms in $B \to X(s\gamma)$ in effective field theory*, *Phys. Rev.* **D 63** (2000) 014006 [hep-ph/0005275] [INSPIRE].

[84] C.W. Bauer, S. Fleming, D. Pirjol and I.W. Stewart, *An effective field theory for collinear and soft gluons: Heavy to light decays*, *Phys. Rev.* **D 63** (2001) 114020 [hep-ph/0011336] [INSPIRE].

[85] C.W. Bauer and I.W. Stewart, *Invariant operators in collinear effective theory*, *Phys. Lett.* **B 516** (2001) 134 [hep-ph/0107001] [INSPIRE].

[86] C.W. Bauer, D. Pirjol and I.W. Stewart, *Soft collinear factorization in effective field theory*, *Phys. Rev.* **D 65** (2002) 054022 [hep-ph/0109045] [INSPIRE].

[87] C.W. Bauer, S. Fleming, D. Pirjol, I.Z. Rothstein and I.W. Stewart, *Hard scattering factorization from effective field theory*, *Phys. Rev.* **D 66** (2002) 014017 [hep-ph/0202088] [INSPIRE].

[88] C.F. Berger, T. Kucs and G.F. Sterman, *Event shape/energy flow correlations*, *Phys. Rev.* **D 68** (2003) 014012 [hep-ph/0303051] [INSPIRE].

[89] A. Hornig, C. Lee and G. Ovanesyan, *Effective predictions of event shapes: factorized, resummed and gapped angularity distributions*, *JHEP* **05** (2009) 122 [arXiv:0901.3780] [INSPIRE].

[90] A. Jain, M. Procura and W.J. Waalewijn, *Fully-unintegrated parton distribution and fragmentation functions at perturbative k_T*, *JHEP* **04** (2012) 132 [arXiv:1110.0839] [INSPIRE].

[91] S. Mantry and F. Petriello, *Factorization and resummation of Higgs boson differential distributions in soft-collinear effective theory*, *Phys. Rev.* **D 81** (2010) 093007 [arXiv:0911.4135] [INSPIRE].

[92] M. Procura, W.J. Waalewijn and L. Zeune, *Resummation of double-differential cross sections and fully-unintegrated parton distribution functions*, *JHEP* **02** (2015) 117 [arXiv:1410.6483] [INSPIRE].

[93] I.W. Stewart, F.J. Tackmann and W.J. Waalewijn, *The quark beam function at NNLL*, *JHEP* **09** (2010) 005 [arXiv:1002.2213] [INSPIRE].

[94] J.-y. Chiu, A. Jain, D. Neill and I.Z. Rothstein, *The rapidity renormalization group*, *Phys. Rev. Lett.* **108** (2012) 151601 [arXiv:1104.0881] [INSPIRE].

JHEP11(2015)072

[95] J.-Y. Chiu, A. Jain, D. Neill and I.Z. Rothstein, *A formalism for the systematic treatment of rapidity logarithms in quantum field theory*, *JHEP* **05** (2012) 084 [arXiv:1202.0814] [INSPIRE].

[96] S. Fleming, A.K. Leibovich and T. Mehen, *Resummation of large endpoint corrections to color-octet J/ψ photoproduction*, *Phys. Rev.* **D 74** (2006) 114004 [hep-ph/0607121] [INSPIRE].

[97] T. Becher, G. Bell and M. Neubert, *Factorization and resummation for jet broadening*, *Phys. Lett.* **B 704** (2011) 276 [arXiv:1104.4108] [INSPIRE].

[98] T. Becher and G. Bell, *NNLL resummation for jet broadening*, *JHEP* **11** (2012) 126 [arXiv:1210.0580] [INSPIRE].

[99] F.J. Tackmann, J.R. Walsh and S. Zuberi, *Resummation properties of jet vetoes at the LHC*, *Phys. Rev.* **D 86** (2012) 053011 [arXiv:1206.4312] [INSPIRE].

[100] T. Becher and M. Neubert, *Factorization and NNLL resummation for Higgs production with a jet veto*, *JHEP* **07** (2012) 108 [arXiv:1205.3806] [INSPIRE].

[101] A. Banfi, P.F. Monni, G.P. Salam and G. Zanderighi, *Higgs and Z-boson production with a jet veto*, *Phys. Rev. Lett.* **109** (2012) 202001 [arXiv:1206.4998] [INSPIRE].

[102] T. Becher, M. Neubert and L. Rothen, *Factorization and N^3LL_p+NNLO predictions for the Higgs cross section with a jet veto*, *JHEP* **10** (2013) 125 [arXiv:1307.0025] [INSPIRE].

[103] I.W. Stewart, F.J. Tackmann, J.R. Walsh and S. Zuberi, *Jet p_T resummation in Higgs production at $NNLL' + NNLO$*, *Phys. Rev.* **D 89** (2014) 054001 [arXiv:1307.1808] [INSPIRE].

[104] T. Becher and X. Garcia i Tormo, *Factorization and resummation for transverse thrust*, *JHEP* **06** (2015) 071 [arXiv:1502.04136] [INSPIRE].

JHEP11(2015)072